Electronic Supplementary Material (ESI) for RSC Advances.

Supporting information for:

Conjugated Anthracene Dendrimers with Monomer-Like Fluorescence

Karl Börjesson, Mélina Gilbert, Damir Dzebo, Bo Albinsson and Kasper Moth-Poulsen

Contents

1. Synthesis

General: Commercially available reagents were used without further purification if not otherwise stated. 1,3,5-tribromobenzene was purified by column chromatography prior to use. Tetrahydrofuran (THF) was dried by distillation over sodium, and deaeration of toluene and tetraethylammonium hydroxide (20 % in water, TEAOH) were achieved by bubbling of nitrogen for 20 minutes. Mass spectroscopy (MALDI) was performed on a Bruker Autoflex (positive mode, *trans*-2-[3-(4-*tert*-butylphenyl)-2-methyl-2-propenylidene]malononitrile matrix) and NMR was performed on an automated Agilent (Varian) MR400 MHz. Elemental analysis was made by H. Kolbe mikroanalytisches laboratorium, Mülheim an der Ruhr, Germany. IR spectra were measured on a Perkin Elmer System 2000 FT-IR.

9-bromo-10-phenyl-antracene: Bromine (5.12 mmol, 0.26 ml) was added drop vise to a reaction vessel containing 9-phenyl-anthracene (5.12 mmol, 1.3 g) dissolved in carbontetrachloride (60 ml) kept at 0 °C. The mixture was allowed to stir at 0 °C for 1 h where after it was poured into an extraction vessel containing dichloromethane and $NaHCO_{3(aq)}$ (5 % solution). The organic phase was washed twice with water where after it was evaporated to dryness. The reaction mixture was recrystalised using toluene to receive 9-bromo-10-phenylanthracene in 90 % yield.

^{1}H NMR (400 MHz, $CDCl_3$) δ=8.61 (dt, J = 8.4, 1.0 Hz, 2H), 7.65 (dt, J = 8.8, 1.0 Hz, 2H), 7.62-7.53 (m, 5H), 7.42-7.35 (m, 4H)^{13}C NMR (100 MHz, $CDCl_3$) δ= 138.4, 137.8, 131.1, 131.0, 130.2, 128.4, 127.8, 127.7, 127.4, 126.9, 125.5, 122.7

Maldi: Calculated for $C_{20}H_{13}Br$ = 332.02, found 331.808

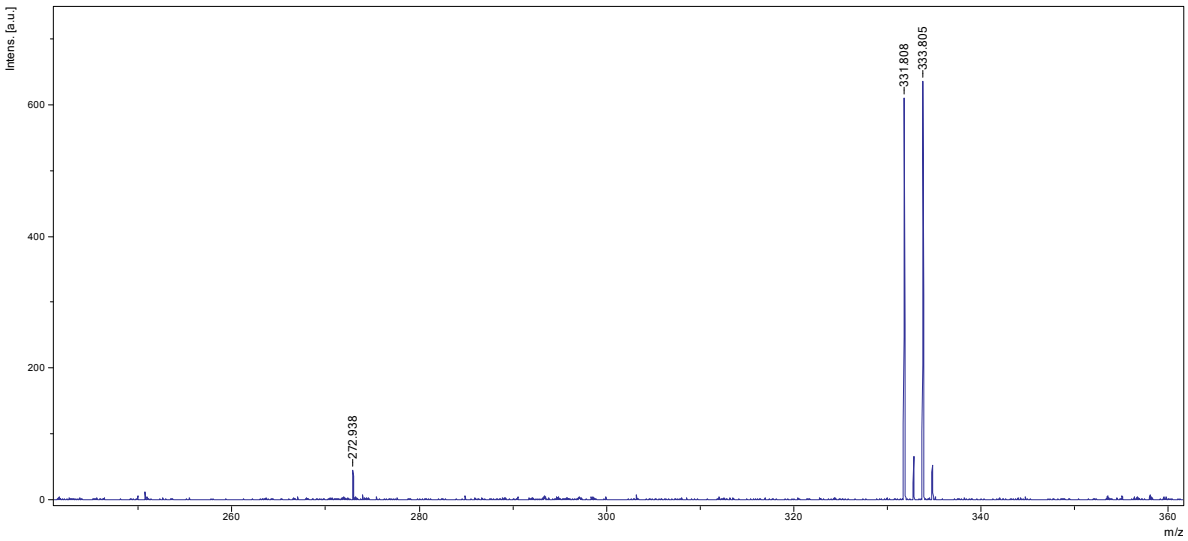

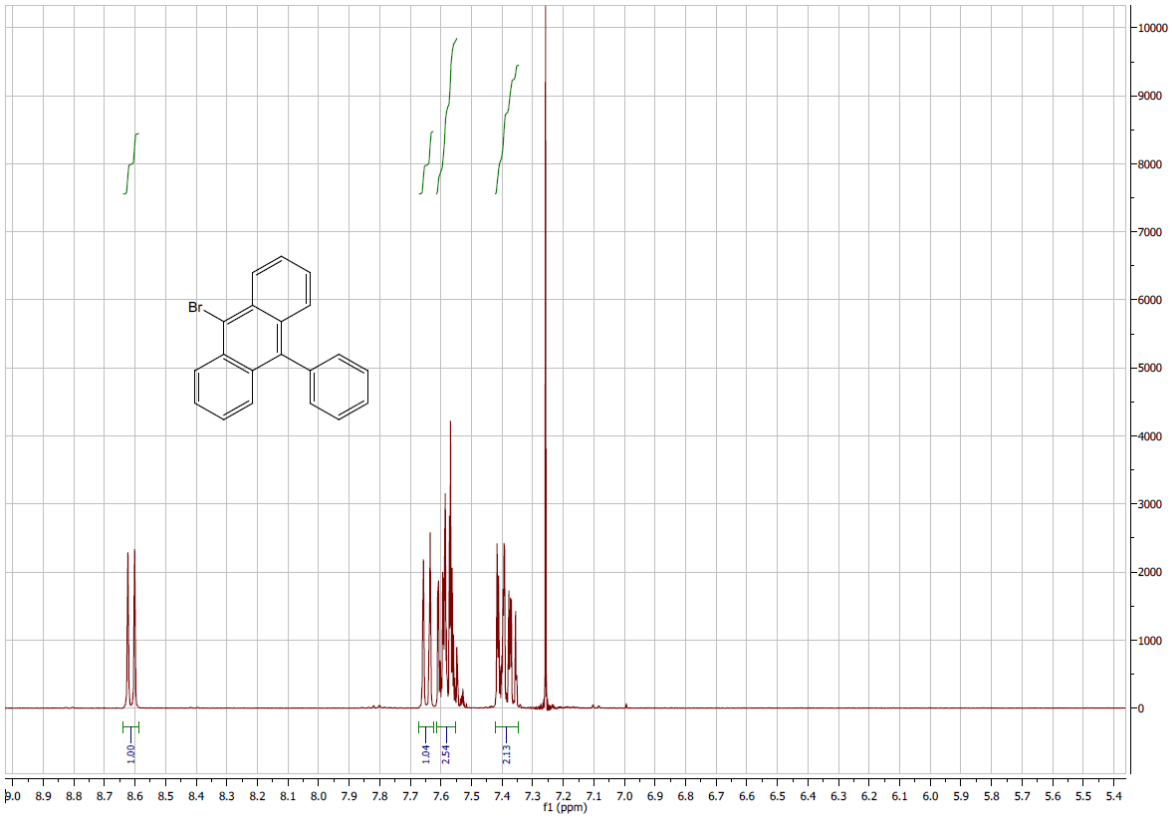
Br
1.00
1.04
2.54
2.13
f1 (ppm)

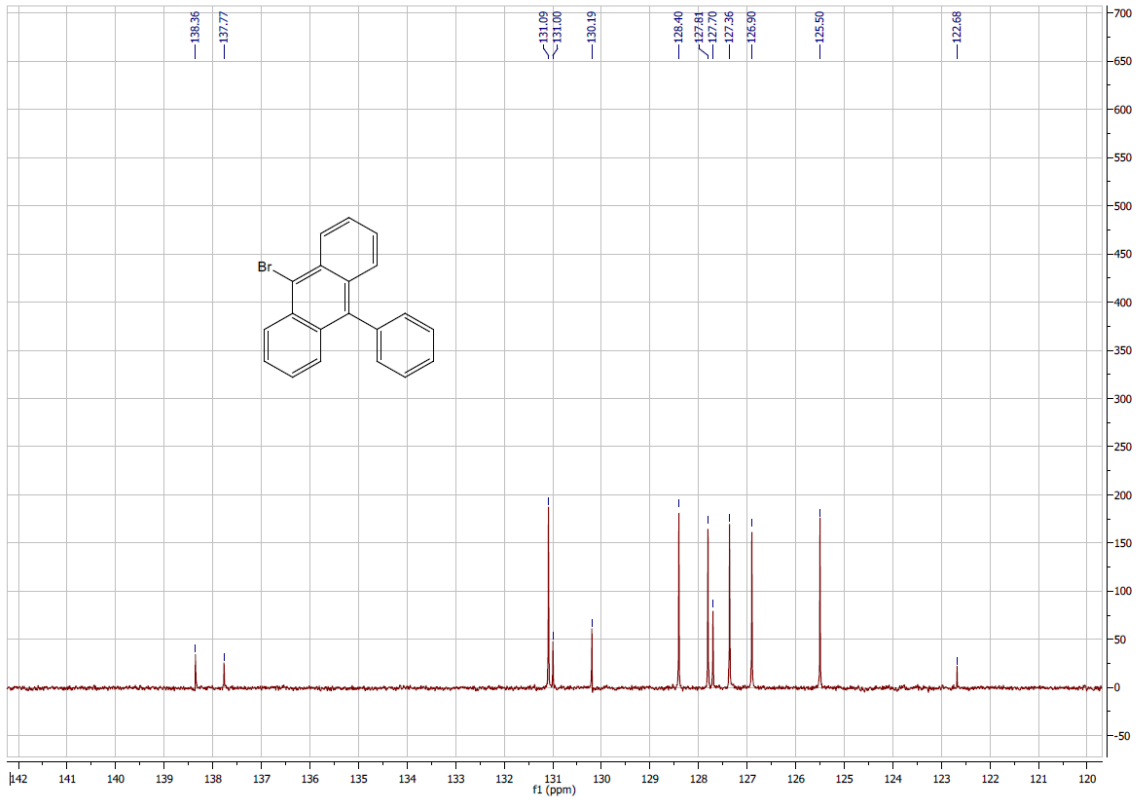
138.36
137.77
131.09
131.00
130.19
128.40
127.81
127.70
127.36
126.90
125.50
122.68
Br
f1 (ppm)

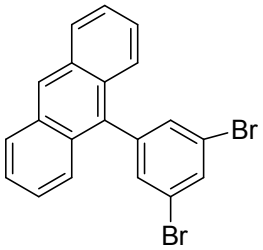

1-anthracene-3,5-bromobenzene: Deaerated toluene (10 ml) and tetraethylammonium hydroxide (20 % in water, 10 ml, 13 mmol) was added to a reaction vessel containing 1,3,5-tribromobenzene (6.6 mmol, 2 g), 9-anthraceneboronic acid bis(pinacol)ester (1.3 mmol, 400 mg), $Pd_2(dba)_3$ (0.066 mmol, 60 mg) and tri(o-tolyl)phosphine (0.26 mmol, 80 mg) kept under nitrogen atmosphere. The reaction mixture was vigorously stirred at 103 °C for 72 h where after it was cooled and poured into an extraction vessel containing water and toluene. The organic phase was washed twice with water and then evaporated to dryness. The crude reaction mixture was purified by column chromatography (silica, hexane) to give 1-anthracene-3,5-bromobenzene slightly contaminated with anthracene in 30 % yield (the anthracene was easily removed in the next step in the reaction pathway).

^{1}H NMR (400 MHz, $CDCl_3$) δ = 8.53 (s, 1 H), 8.05 (m, 2H), 7.86 (t, J = 1.8 Hz, 1H), 7.59 (m, 2H), 7.54 (d, J = 1.8 Hz, 2H), 7.51-7.38 (m, 4H)

^{13}C NMR (100 MHz, $CDCl_3$) δ = 142.6, 133.3, 133.2, 132.9, 131.1, 129.9, 128.5, 127.6, 126.1, 126.0, 125.3, 123.0

Maldi: Calculated for $C_{20}H_{12}Br_2$ = 411.93, found 411.755

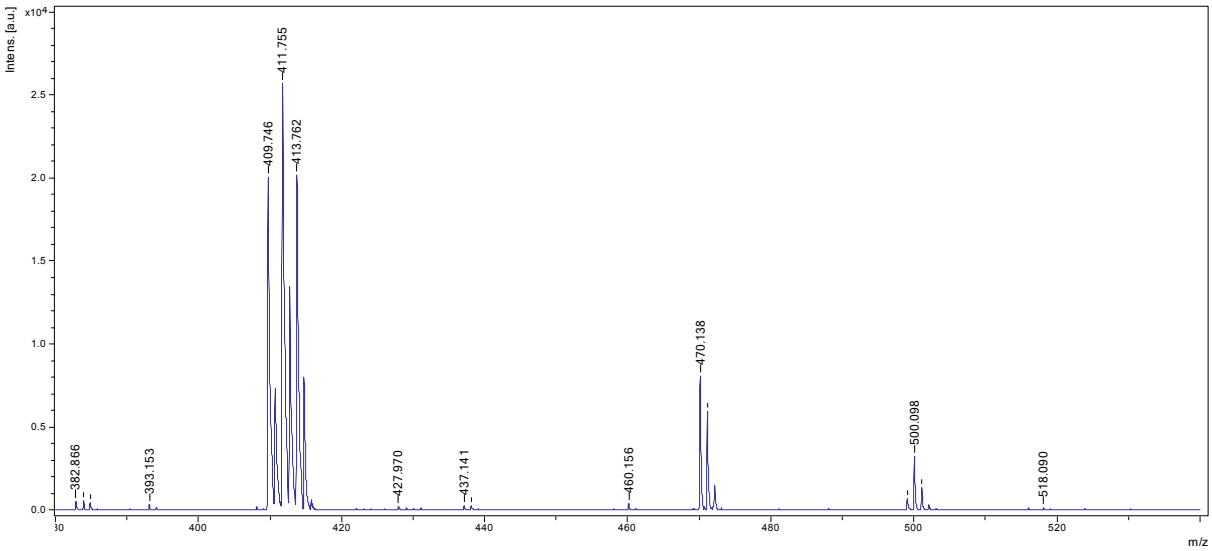

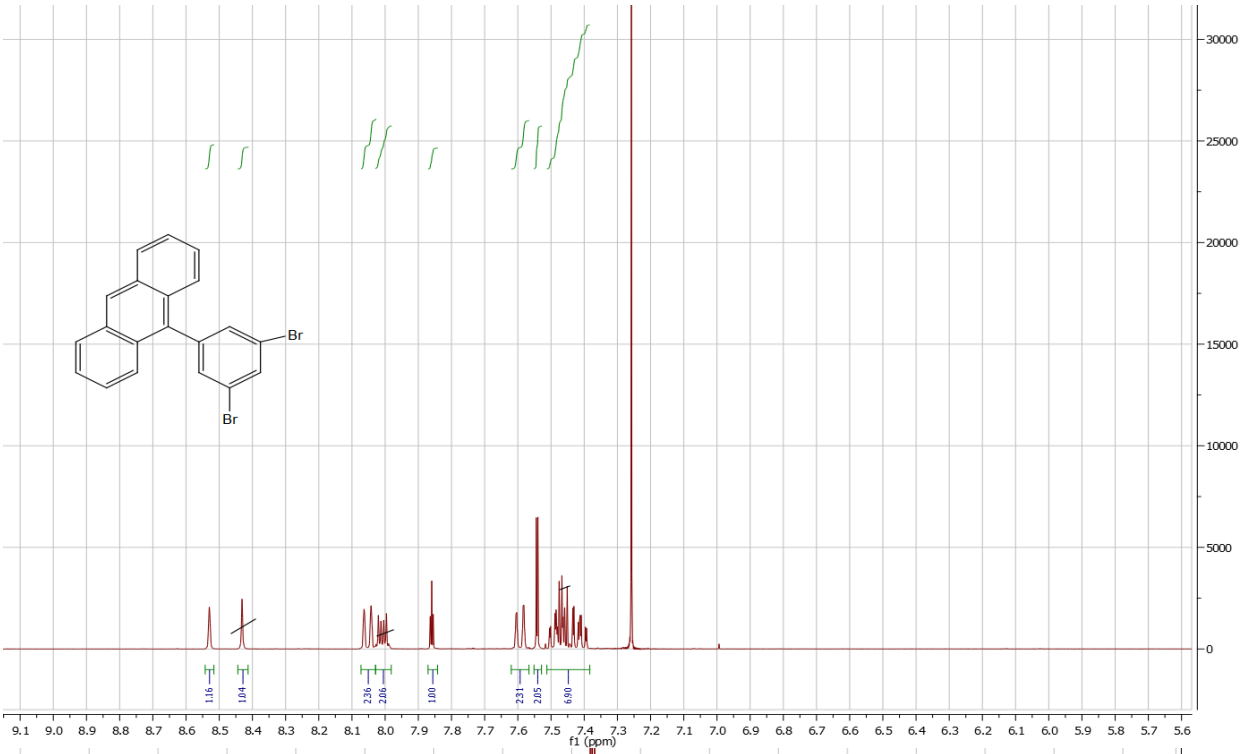
Br
Br
1.16
1.04
2.36
2.06
1.00
2.31
2.05
6.90
f1 (ppm)

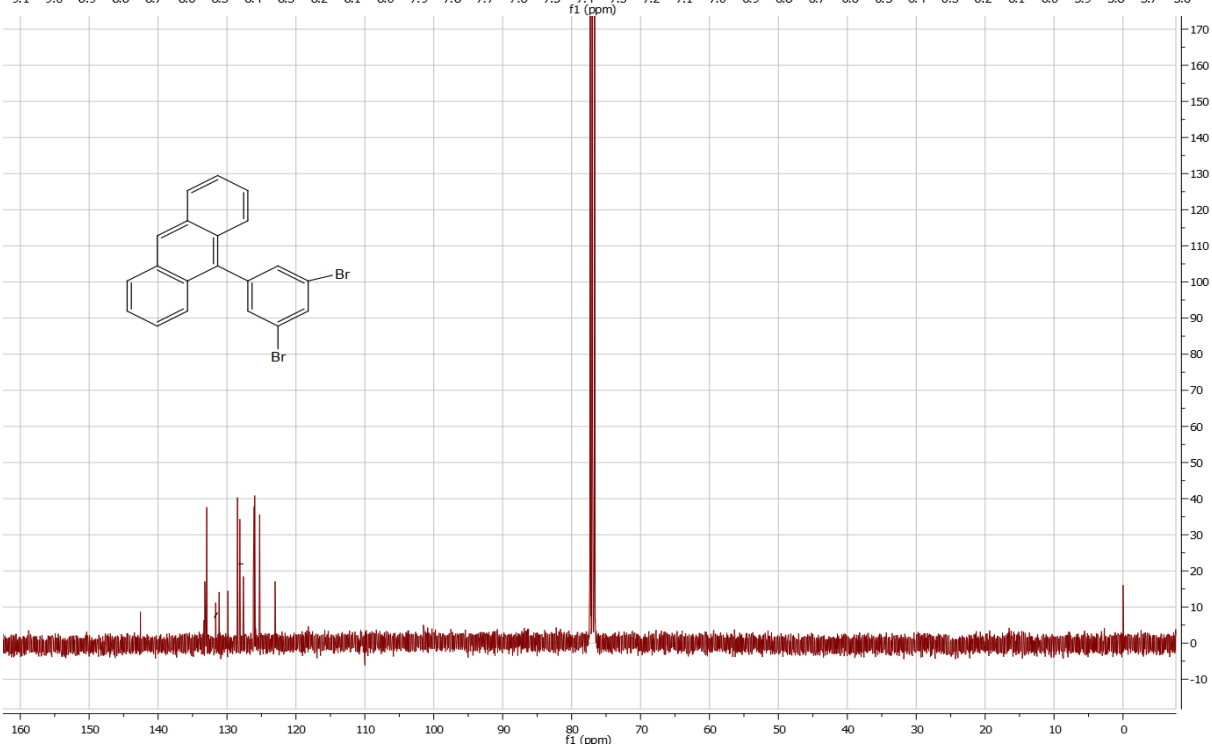
Br
Br
f1 (ppm)

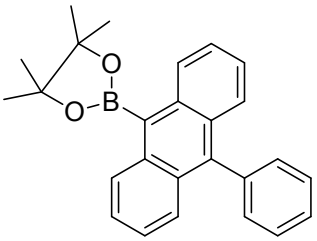

10-phenyl-9-anthracenylboronic acid pinacol ester: Tert-butyllithium (1.8 mmol, 1.06 ml) was added drop vise to a vessel containing 9-bromo-10-phenylanthracene (0.9 mmol, 300 mg) and dry THF (9 ml) kept under nitrogen atmosphere at -80 °C. The reaction mixture was stirred at -80 °C for 1 h where after 2-Isopropoxy-4,4,5,5-tetramethyl-1,3,2-dioxaborolane (1.8 mmol, 0.37 ml) was added and the reaction vessel was slowly allowed to heat up to room temperature over 16 h. The reaction mixture was poured into an extraction vessel containing dichloromethane and water, and the organic phase was washed two times with water and then evaporated to dryness. The resultant mixture was purified by column chromatography (silica, hexan/DCM 1:1) to give 10-phenyl-9-anthracenylboronic acid pinacol ester in 86 % yield.

^{1}H NMR (400 MHz, $CDCl_3$) δ = 8.44 (d, J = 8.8 Hz, 2 H), 7.63 (d, J = 8.8 Hz, 2 H), 7.60-7.28 (m, 9 H), 1.60 (s, 12 H)

^{13}C NMR (100 MHz, $CDCl_3$) δ = 139.5, 139.1, 135.4, 131.1, 129.7, 128.4, 128.3, 127.4, 125.4, 124.8, 84.5, 25.2

Maldi: Calculated for $C_{26}H_{25}BO_2$ = 380.19, found 379.91

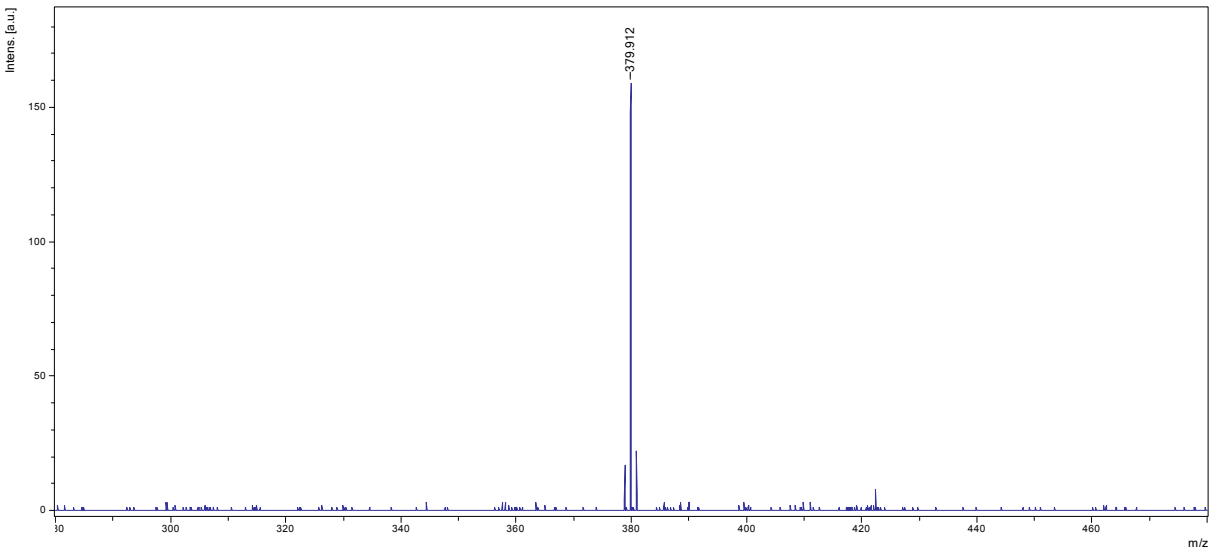

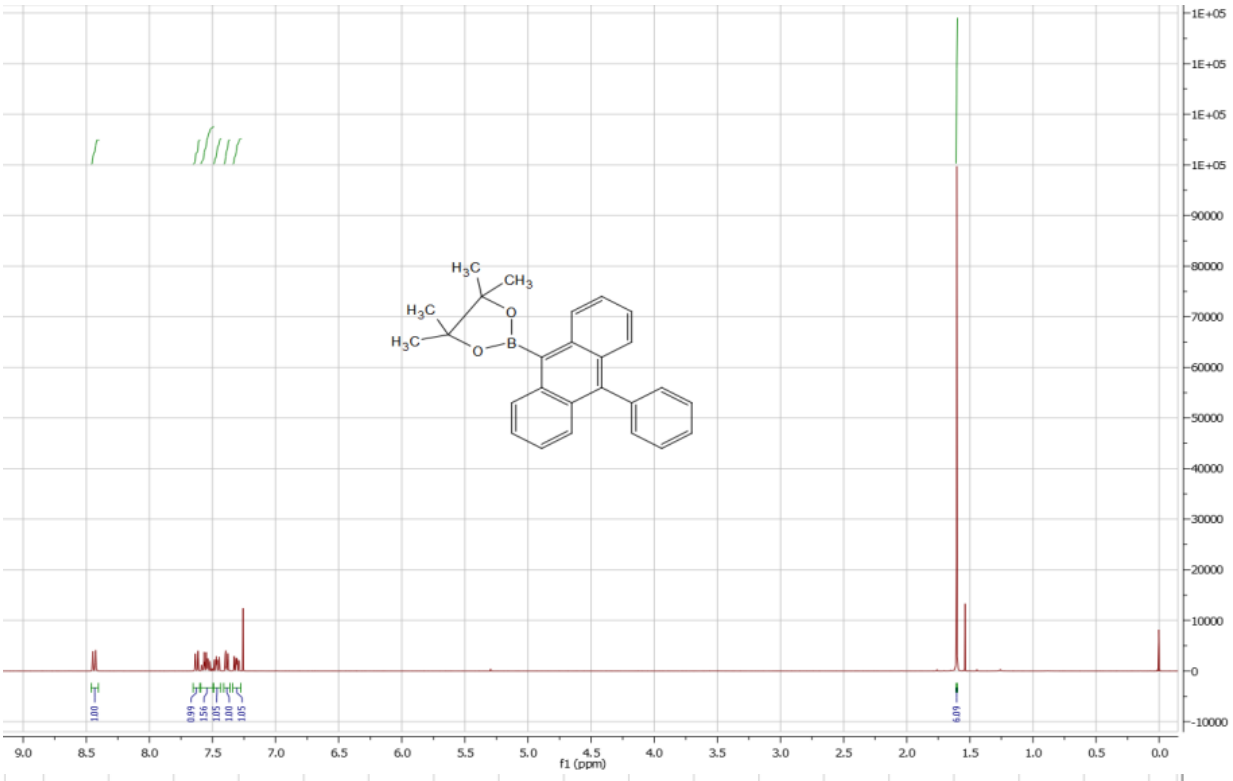
f1 (ppm)

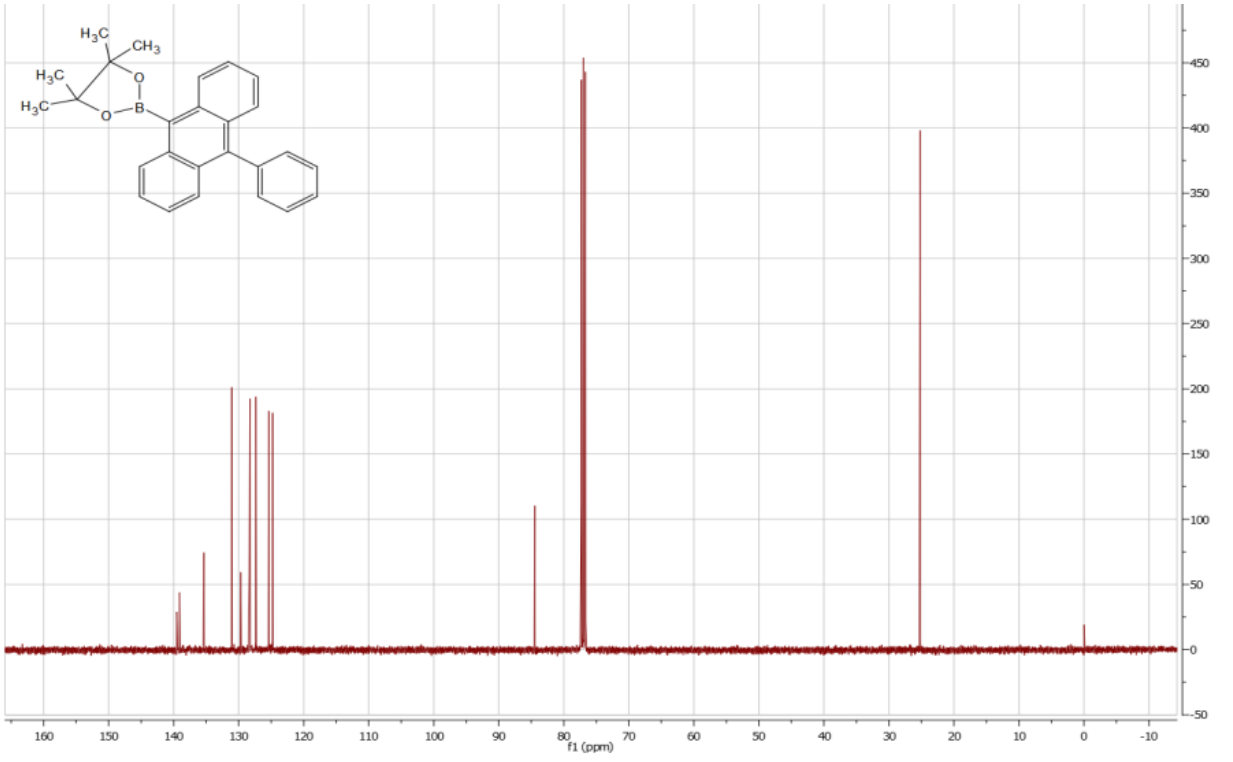
f1 (ppm)

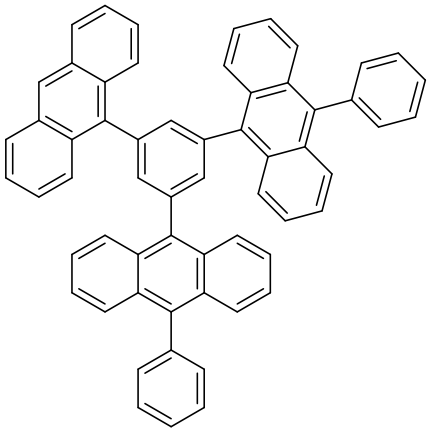

1,3-bis(9-phenylanthracen-10-yl)-5-(antracen-9-yl)-benzene: Deaerated toluene (6 ml) and tetraethylammonium hydroxide (20 % in water, 6 ml, 7.8 mmol) was added to a reaction vessel containing 1-anthracene-3,5-bromobenzene (0.2 mmol, 80 mg), 10-phenyl-9-anthracenylboronic acid pinacol ester (0.8 mmol, 300 mg), $Pd_2(dba)_3$ (0.039 mmol, 36 mg) and tri(o-tolyl)phosphine (0.16 mmol, 47 mg) kept under nitrogen atmosphere. The reaction mixture was heated up to 103 °C and vigorously stirred for 72 h where after it was cooled and poured into an extraction vessel containing water and toluene. The organic phase was washed twice with water and then evaporated to dryness. The crude reaction mixture was purified by column chromatography (silica, hexane/DCM 4/1) to give 1,3-bis(9-phenylanthracen-10-yl)-5-(antracen-9-yl)-benzene in 94 % yield.

^{1}H NMR (400 MHz, $CDCl_3$) δ = 8.52 (s, 1 H), 8.25 (m, 6 H), 8.06 (d, J = 8.8 Hz, 2 H), 7.87 (t, J = 1.6 Hz, 1 H), 7.84 (d, J = 1.6 Hz, 2 H), 7.70 (m, 4 H), 7.65-7.30 (m, 22 H)

^{13}C NMR (100 MHz, $CDCl_3$) δ = 139.2, 139.0, 138.9, 137.5, 136.3, 136.2, 133.9, 133.9, 131.4, 131.3, 130.3, 130.0, 129.9, 128.5, 128.4, 127.5, 127.2, 126.9, 126.7, 126.6, 125.8, 125.4, 125.1, 125.0

Maldi: Calculated for $C_{60}H_{38}$ = 758.30, found 757.65

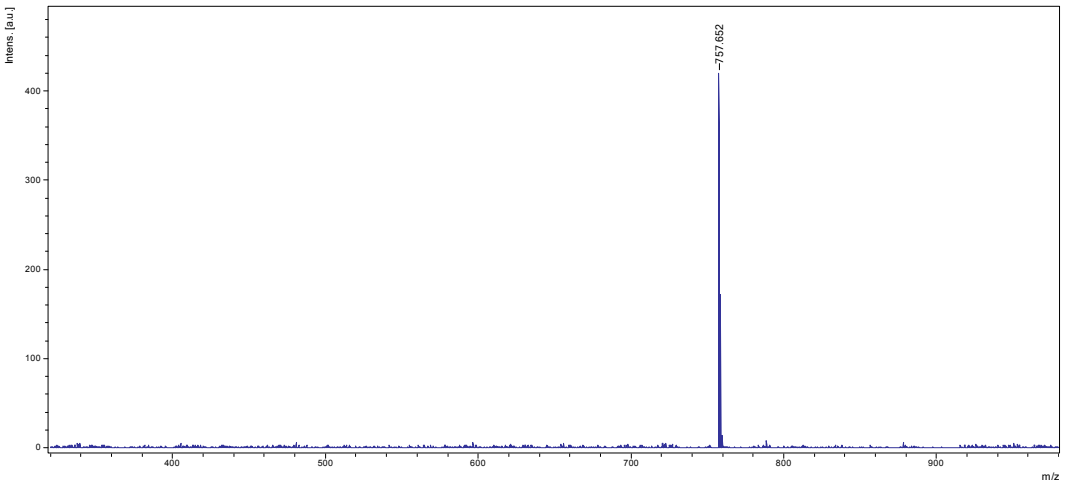

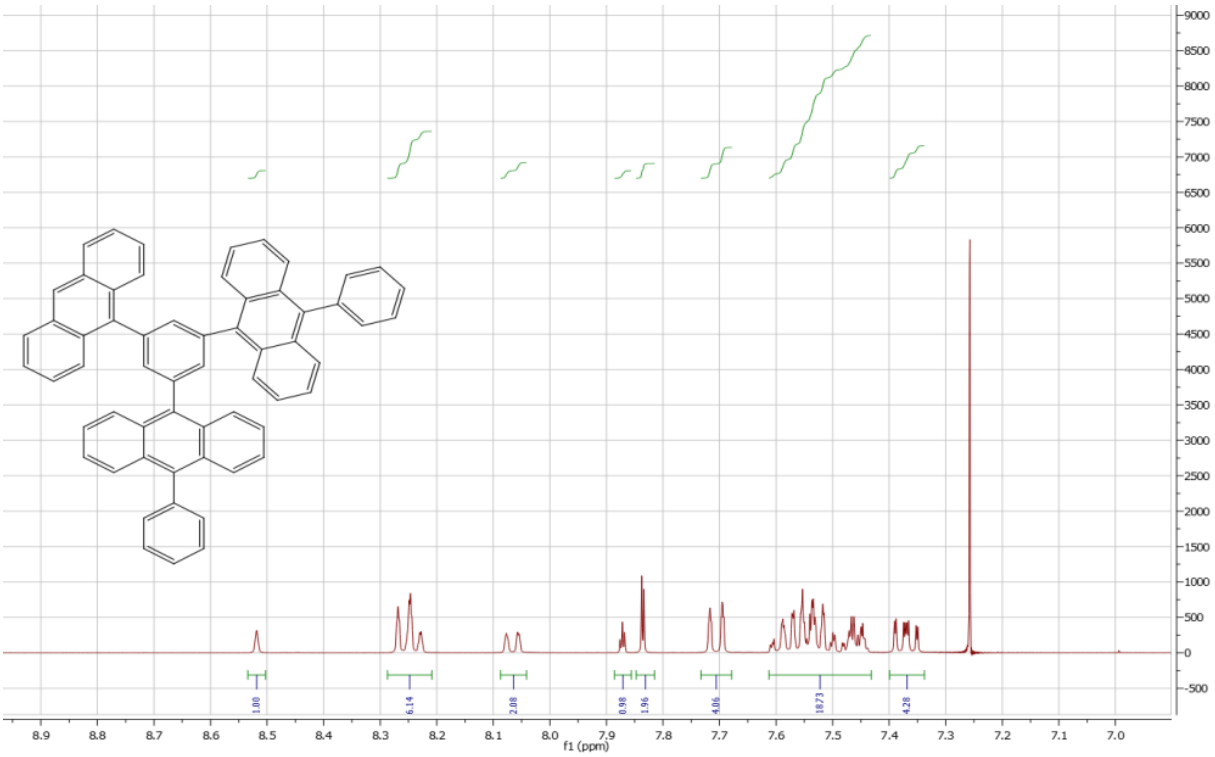
1.00
6.14
2.08
0.98
1.96
4.06
18.73
4.28
f1 (ppm)

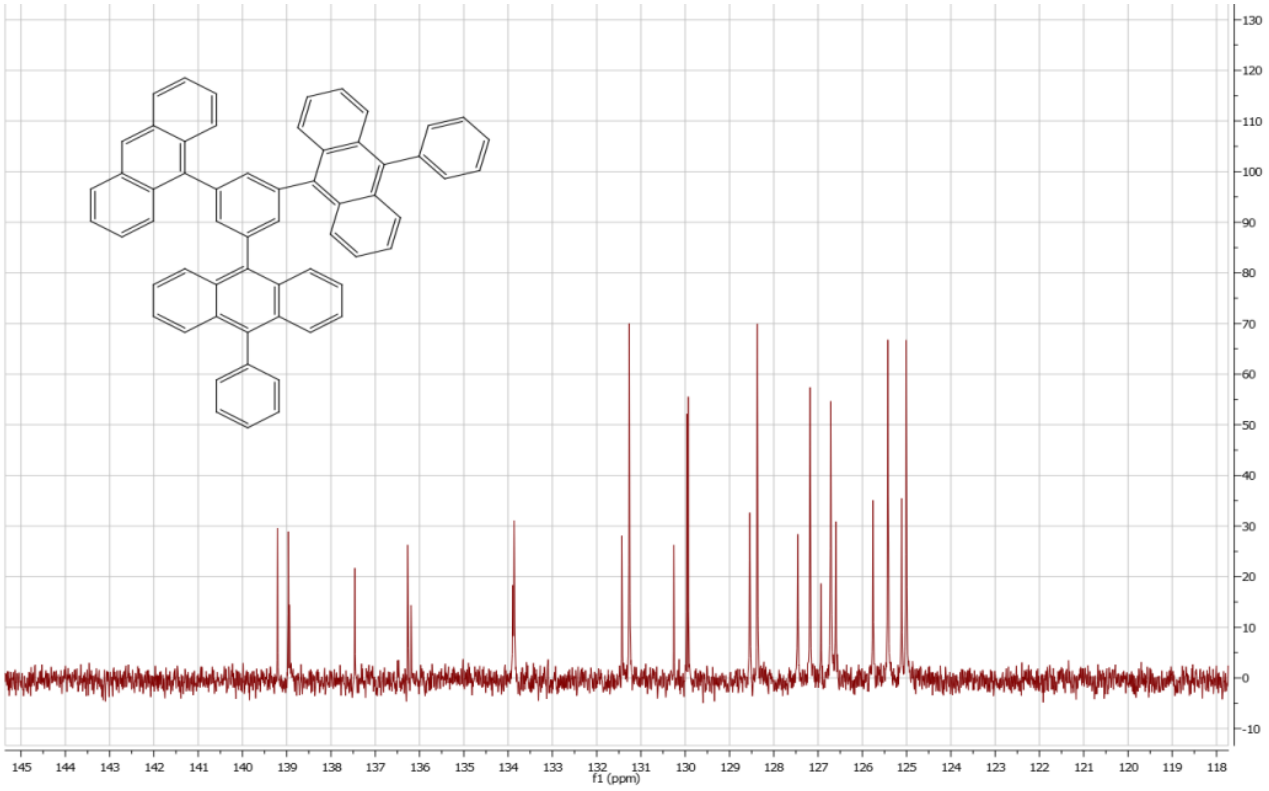
f1 (ppm)

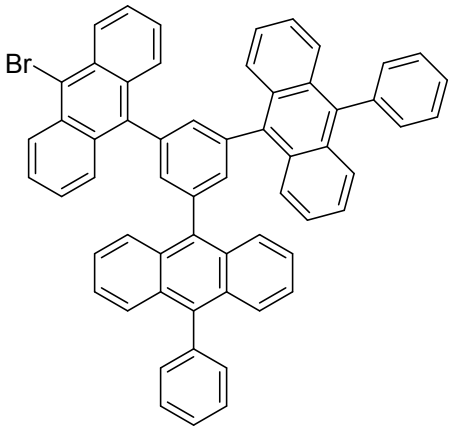

1-(9-bromoantracen-10-yl)-3,5-bis(9-phenylanthracen-10-yl)-benzene: Bromine (1.075 mmol, 55 µl) was added drop vise to a reaction vessel containing 1,3-bis(9-phenylanthracene-10-yl)-5-(antracen-9-yl)-benzene (1.075 mmol, 816 mg) dissolved in carbontetrachloride (15 ml) kept at 0 °C. The mixture was allowed to stir at 0 °C for 1 h where after it was poured into an extraction vessel containing dichloromethane and $NaHCO_{3(aq)}$ (5 % solution). The organic phase was washed twice with water where after it was evaporated to dryness. The reaction mixture was redisolved in dichloromethane and crystallized by carefully adding methanol on top of the dichloromethane layer and left over night. This procedure was repeated and gave 1-(9-bromoantracen-10-yl)-3,5-*bis*(9-phenylanthracen-10-yl)-benzene in 84 % yield.

^{1}H NMR (400 MHz, $CDCl_3$) δ = 8.65 (m, 2H), 8.25 (d, J = 8.2 Hz,6H), 7.91 (t, J = 1.6, 1 H), 7.82 (d, J = 1.6, 2 H), 7.72 (d, J = 8.8 Hz, 4 H), 7.68-7.34 (m, 22 H)

^{13}C NMR (100 MHz, $CDCl_3$) δ = 139.4, 138.9, 138.6, 137.6, 137.0, 136.0, 134.2, 133.8, 131.3, 131.1, 130.3, 130.0, 129.9, 128.4, 128.1, 127.5, 127.3, 127.0, 126.6, 126.0, 125.5, 125.0, 123.2

Maldi: Calculated for $C_{60}H_{37}Br$ = 838.21, found 837.976

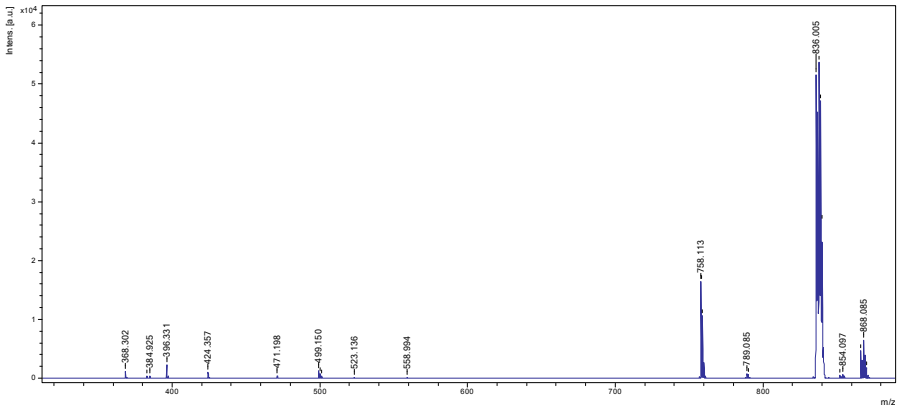

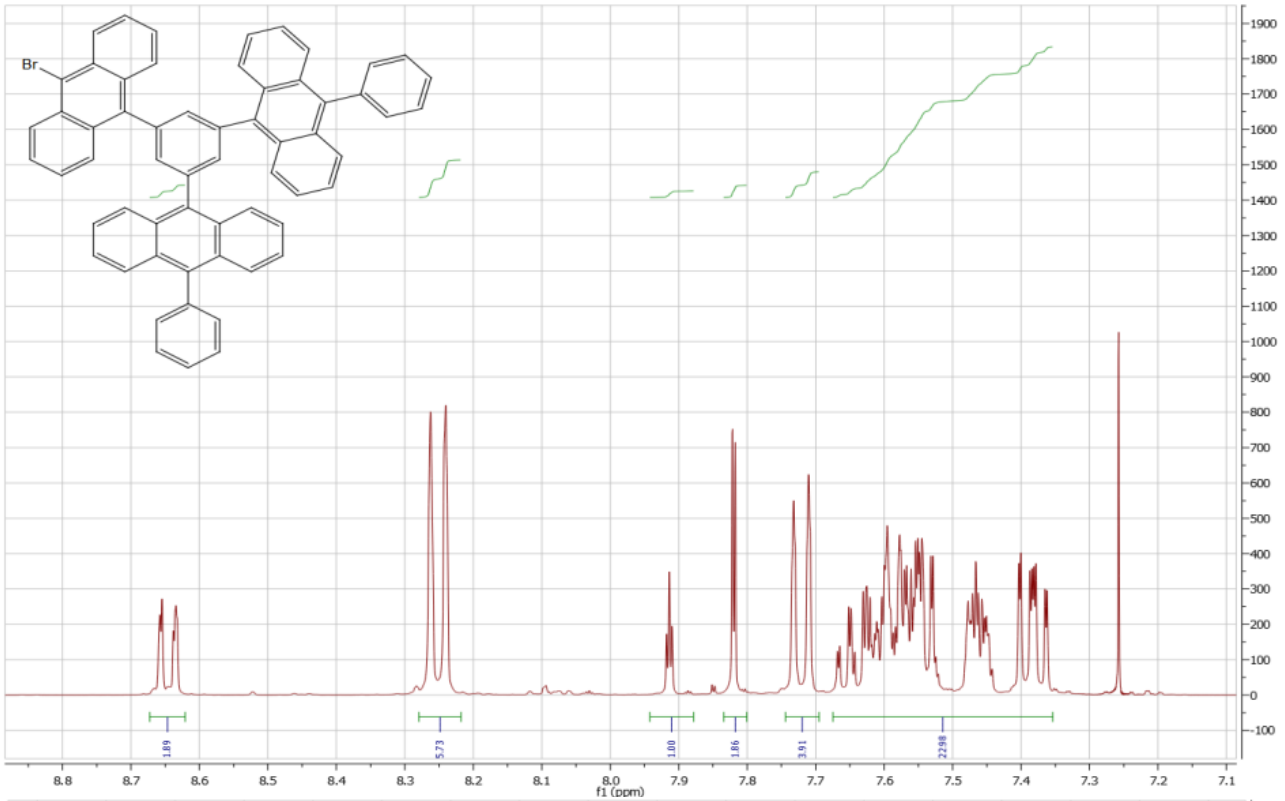
Br
1.89
5.73
1.00
1.86
3.91
22.98
f1 (ppm)

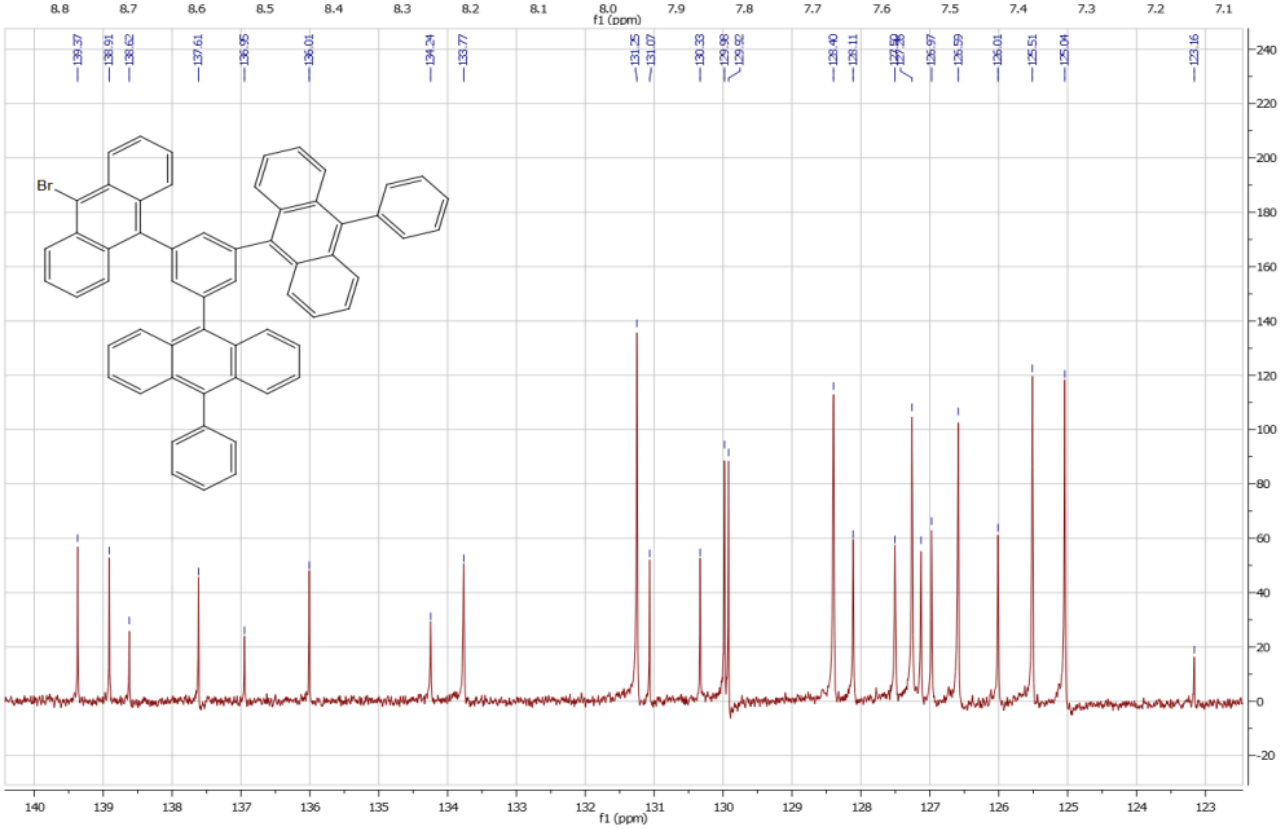
Br
139.37
138.91
138.62
137.61
136.95
136.01
134.24
133.77
131.25
131.07
130.33
129.98
129.92
128.40
128.11
127.80
127.38
126.97
126.59
126.01
125.51
125.04
123.16
f1 (ppm)

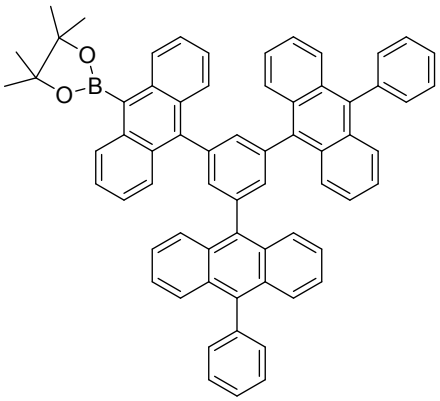

1-(9-anthracen-10-ylboronic acid pinacol ester)-3,5-bis(9-phenylanthracen-10-yl)-benzene: Tert-butyllithium (0.92 mmol, 0.54 ml) was added drop vise to a vessel containing 1-(9-bromoantracen-10-yl)-3,5-*bis*(9-phenylanthracen-10-yl)-benzene (0.46 mmol, 384 mg) and dry THF (15 ml) kept under nitrogen atmosphere at -80 °C. The reaction mixture was stirred at -80 °C for 1 h where after 2-Isopropoxy-4,4,5,5-tetramethyl-1,3,2-dioxaborolane (0.92 mmol, 0.19 ml) was added and the reaction vessel was slowly allowed to heat up to room temperature over 16 h. The reaction mixture was poured into an extraction vessel containing dichloromethane and water, and the organic phase was washed two times with water and then evaporated to dryness. The resultant mixture was purified by column chromatography (silica, hexan/DCM 1:1) to give the boronic ester in 73 % yield.

^{1}H NMR (400 MHz, $CDCl_3$) δ = 8.47 (m, 2 H), 8.25 (m, 6 H), 7.88 (t, J = 1.6 Hz, 1 H), 7.81 (d, J = 1.6 Hz, 2 H), 7.72 (d, J = 8.8 Hz, 4 H), 7.54 (m, 18 H), 7.38 (m, 4 H), 1.60 (s, 12 H)

^{13}C NMR (100 MHz, $CDCl_3$) δ = 139.3, 139.2, 139.0, 138.7, 137.5, 136.3, 135.5, 133.9, 133.7, 131.3, 131.3, 130.0, 130.0, 129.8, 128.6, 128.4, 128.4, 127.5, 127.2, 126.7, 125.5, 125.3, 125.0, 84.5, 25.2

Maldi: Calculated for $C_{66}H_{49}BO_2$ = 884.38, found 884.216

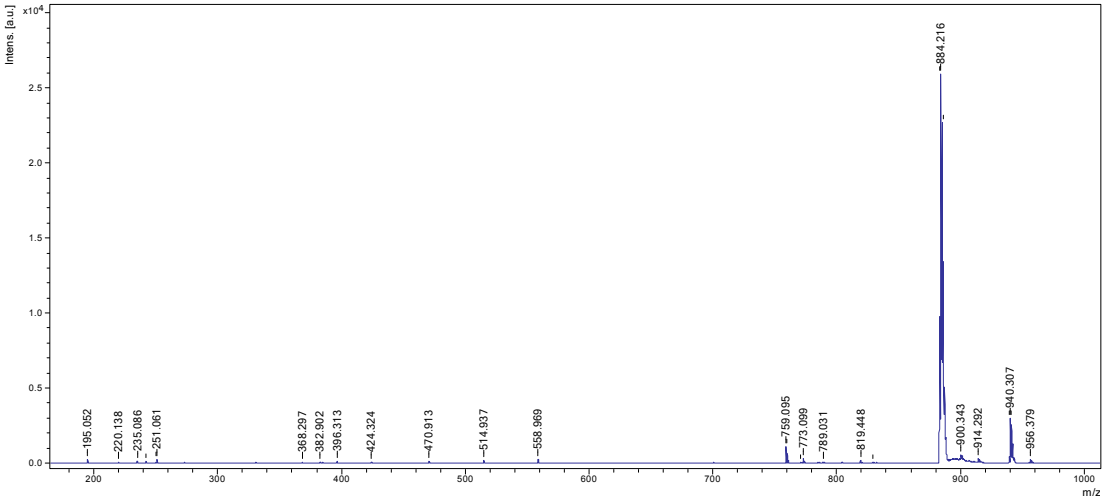

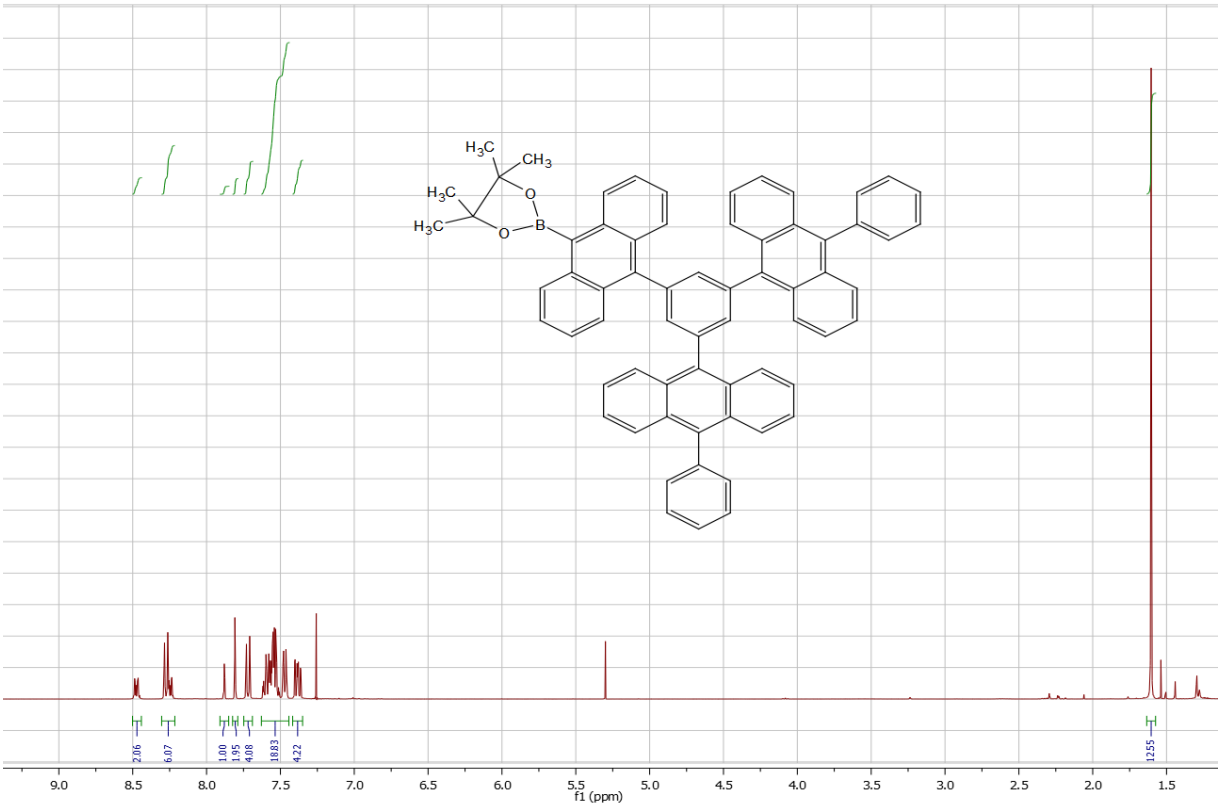
H3C
CH3
H3C
O
H3C
O
B
2.06
6.07
1.00
1.95
4.08
18.83
4.22
12.55
9.0
8.5
8.0
7.5
7.0
6.5
6.0
5.5
5.0
4.5
4.0
3.5
3.0
2.5
2.0
1.5
f1 (ppm)

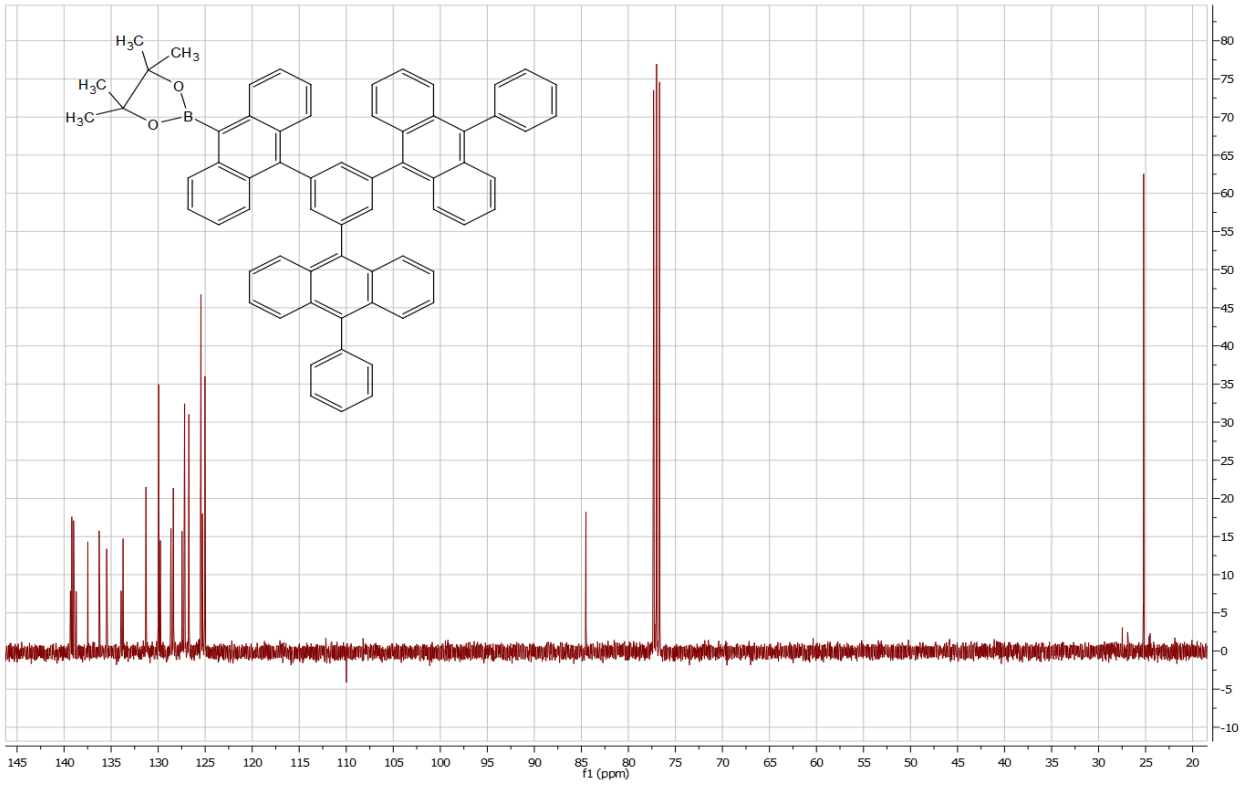
H3C
CH3
H3C
O
H3C
O
B
80
75
70
65
60
55
50
45
40
35
30
25
20
15
10
5
0
-5
-10
145
140
135
130
125
120
115
110
105
100
95
90
85
80
75
70
65
60
55
50
45
40
35
30
25
20
f1 (ppm)

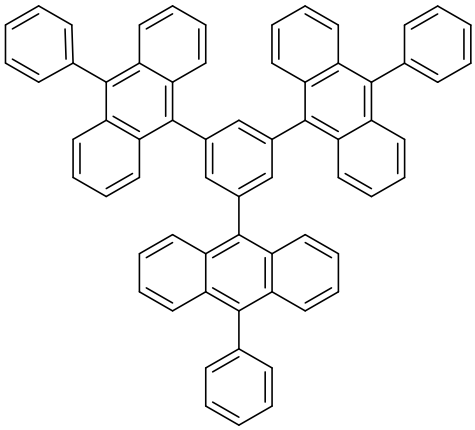

1,3,5-tri(9-phenylanthracen-10-yl)-benzene (G1): Deaerated toluene (6 ml) and tetraethylammonium hydroxide (20 % in water, 6 ml, 8.6 mmol) was added to a reaction vessel containing 1,3,5-tribromobenzene (0.16 mmol, 49 mg), 10-phenyl-9-anthracenylboronic acid pinacol ester (0.86 mmol, 326 mg), $Pd_2(dba)_3$ (0.043 mmol, 39 mg) and tri(o-tolyl)phosphine (0.17 mmol, 52 mg) kept under nitrogen atmosphere. The reaction mixture was heated up to 103 °C and vigorously stirred for 72 h where after it was cooled and poured into an extraction vessel containing water and toluene. The organic phase was washed twice with water and then evaporated to dryness. The crude reaction mixture was purified by column chromatography (silica, hexane/DCM 4/1) to give 1,3,5-tri(9-phenylanthracen-10-yl)-benzene in 89 % yield.

^{1}H NMR (400 MHz, $CDCl_3$) δ = 8.28 (m, 6 H), 7.90 (s, 3 H), 7.71 (m, 6 H), 7.56 (m, 15 H), 7.47 (m, 6 H), 7.38 (m, 6 H)

^{13}C NMR (100 MHz, $CDCl_3$) δ = 139.2, 139.0, 137.5, 136.3, 134.0, 131.3, 130.0, 129.9, 128.4, 127.5, 127.2, 126.7, 125.4, 125.0

Maldi: Calculated for $C_{66}H_{42}$ = 834.33, found 834.164

Elemental analysis calculated for [$C_{66}H_{42}$]:C, 94.25; H, 5.07, found: C, 94.25; H, 5.02.

IR (KBr): 3059 (m), 1585 (w), 1519 (w), 1497 (w), 1439 (m), 1372 (m), 1027 (m), 922 (m), 770 (s), 757 (s), 701 (s), 672 (w), 652 (m), 639 (w), 614 (m) cm^{-1}.

Melting point 228-241 °C.

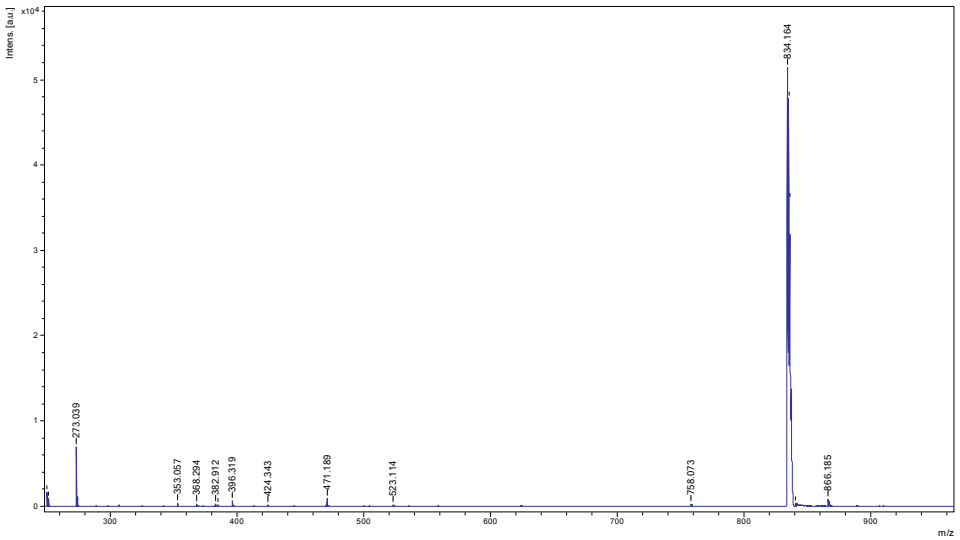

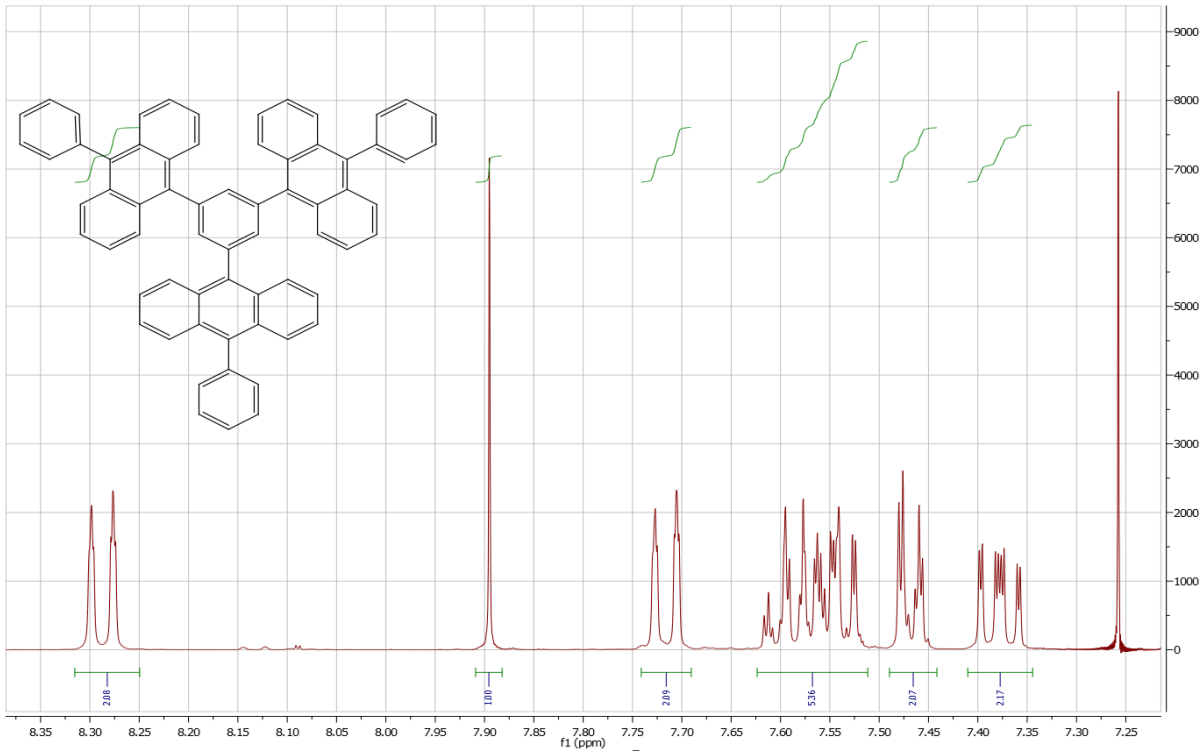
2.08
1.00
2.09
5.36
2.07
2.17
f1 (ppm)

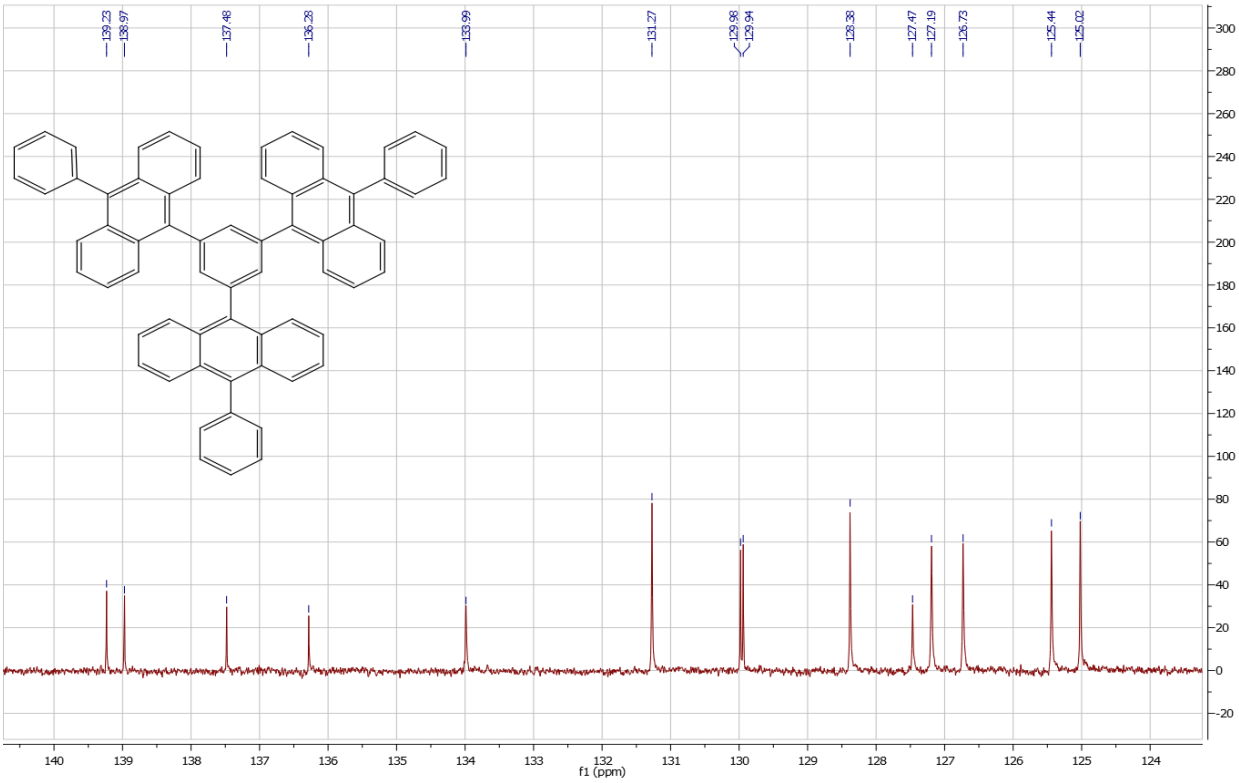
139.23
138.97
137.48
136.29
133.99
131.27
129.98
129.94
128.38
127.47
127.19
126.73
125.44
125.02
f1 (ppm)

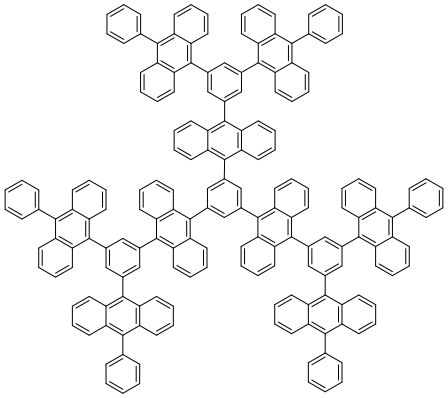

G2: Deaerated toluene (8 ml) and tetraethylammonium hydroxide (20 % in water, 4 ml, 5.5 mmol) was added to a reaction vessel containing 1,3,5-tribromobenzene (0.09 mmol, 29 mg), 1-(9-anthracen-10-ylboronic acid pinacol ester)-3,5-bis(9-phenylanthracen-10-yl)-benzene (0.46 mmol, 404 mg), $Pd_2(dba)_3$ (0.027 mmol, 25 mg) and tri(o-tolyl)phosphine (0.11 mmol, 33 mg) kept under nitrogen atmosphere. The reaction mixture was heated up to 103 °C and vigorously stirred for 72 h where after it was cooled and poured into an extraction vessel containing water and toluene. The organic phase was washed twice with water and then evaporated to dryness. The crude reaction mixture was purified by column chromatography (silica, hexane/DCM 4/1 → pure DCM), followed by precipitation of a dichloromethane solution by methanol, followed by crystallization (hexane/toluene mixture) to give G2 in 50 % yield.

Maldi: Calculated for $C_{186}H_{114}$ = 2347.9, found 2346.96

^{1}H NMR (400 MHz, $CDCl_3$) δ = 8.27 (m, 12 H), 7.84 (m, 12 H), 7.67 (d, J = 8.8 Hz, 12 H), 7.60-7.38 (m, 54 H), 7.33 (m, 12 H).

^{13}C NMR (100 MHz, $CDCl_3$) δ = 139.3, 139.3, 139.2, 139.0, 137.5, 136.7, 136.7, 136.3, 134.1, 134.1, 134.0, 131.3, 130.1, 130.0, 130.0, 128.4, 127.5, 127.2, 127.0, 126.8, 125.6, 125.6, 125.5, 125.0.

Elemental analysis calculated for [$C_{186}H_{114}$]:C, 95.11; H, 4.89, found: C, 93.95; H, 5.59.

IR (KBr): 3061 (m), 1585 (w), 1519 (w), 1441 (m), 1365 (m), 1028 (w), 922 (w), 784 (s), 766 (vs), 729 (w), 702 (s), 653 (m), 639 (w), 612 (w) cm^{-1}.

Degrades before melting (Turns brown at 220 °C).

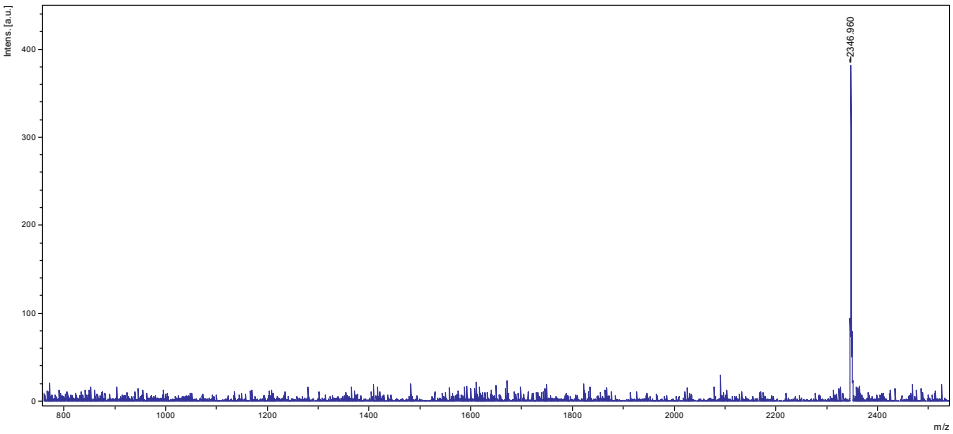

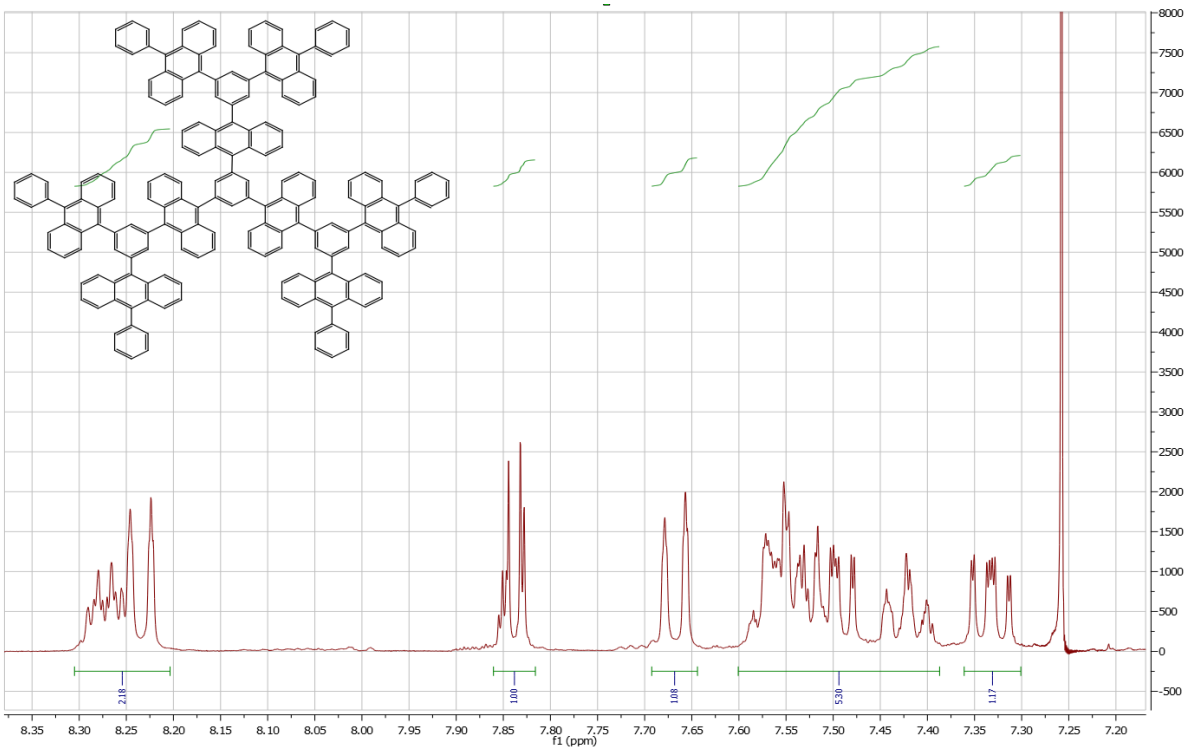
2.18
1.00
1.08
5.30
1.17
f1 (ppm)

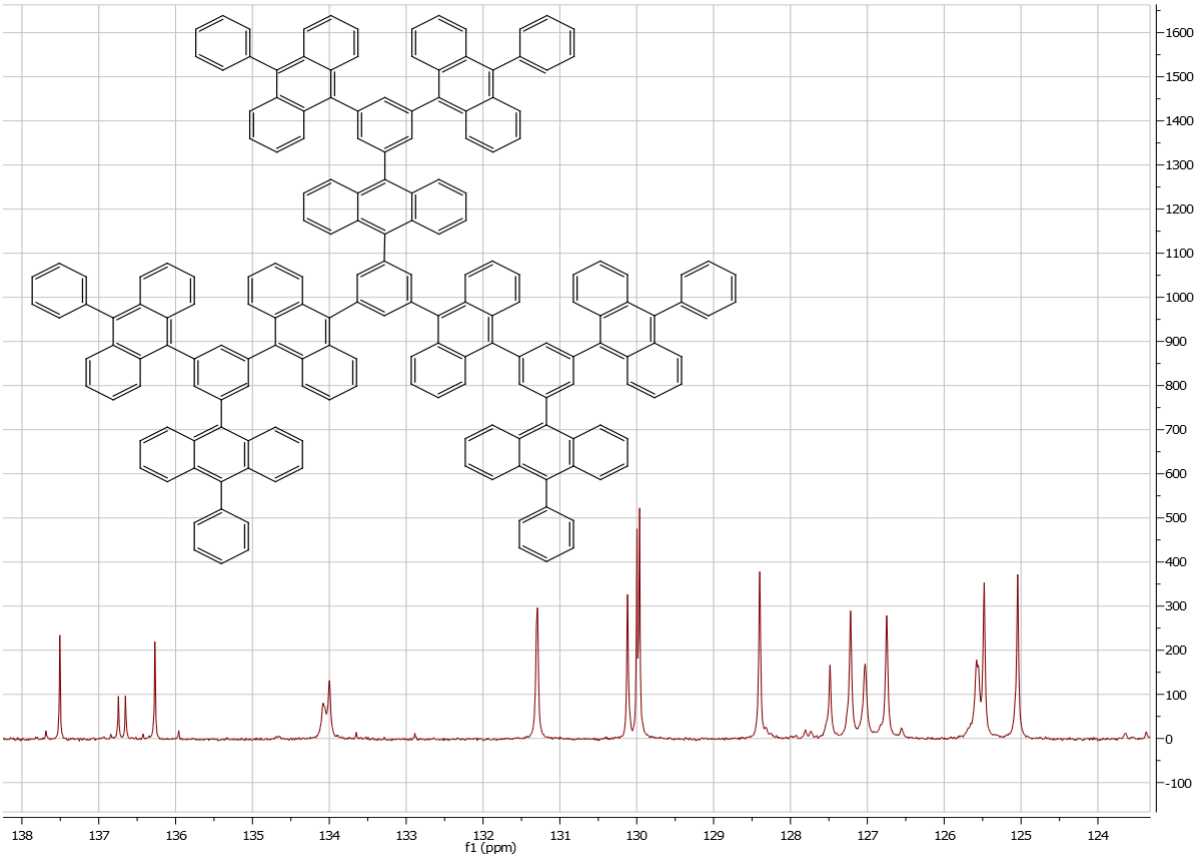
f1 (ppm)

2. Fluorescence quantum yield and lifetimes

The fluorescence quantum yields and lifetimes of DPA, G1 and G2 given in Table S1 were measured in Argon-purged toluene. Toluene was purchased from Sigma-Aldrich (spectrophotometric grade).

The fluorescence quantum yields were determined using DPA in cyclohexane as reference (Φ_{fR} = 0.97) with λ_{exc} 354 nm.[1] The absorbance of all samples was set to < 0.04 at the excitation wavelength. Emission spectra were recorded between 370 nm and 700 nm on a Spex Fluorolog 3 spectrofluorometer (JY Horiba). The quantum yields were calculated according to[2]

$$\Phi_f = \Phi_{fR}\frac{I\ OD_R n^2}{I_R\ OD\ n_R^2} \quad (1)$$

where Φ_f is the fluorescence quantum yield, I is the integrated emission intensity, OD is the optical density and n is the refractive index of the solvent. The reference sample parameters are denoted with subscript R.

Fluorescence lifetimes of DPA and the dendrimers were measured using a time-correlated single photon counting (TCSPC) set up. The excitation pulse (1-2 ps broad) was provided at a repetition rate of 82 MHz by a Tsunami Ti:Sapphire laser (Spectra Physics) that was pumped by a Millenia Pro X laser (Spectra Physics). The tsunami output was set to 770 nm and its repetition rate was subsequently reduced to 4 MHz using a pulse picker (Spectra Physics, Model 3985) before frequency-doubling to yield λ_{exc} 385 nm as excitation wavelength. The emitted photons were collected at magic angle (54.7°) at 430 nm by a micro-channel plate photomultiplier tube (MCP-PMT R3809U-50; Hamamatsu) with a spectral bandwidth of 6 nm. The signal was digitalized using a multi-channel analyzer with 4096 channels (SPC-300, Edinburgh Analytical Instruments) and to get a good statistics 10 000 counts in the top channel were recorded. The measured fluorescence decays of DPA, G1 and G2 shown in Figure S1 were fitted to mono-exponential expressions using the program FluoFit Pro v.4 (PicoQuant GmbH) after deconvolution of the data with the instrument response function (IRF).

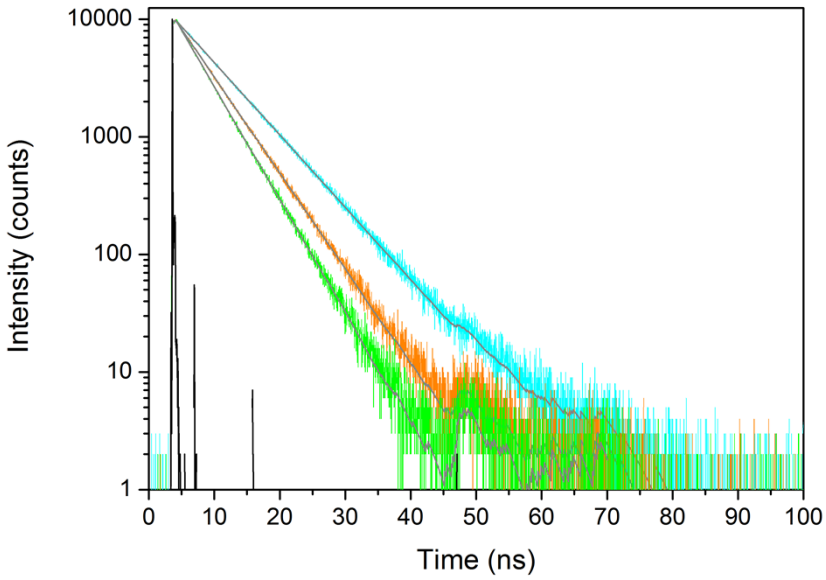

Figure S1. Fluorescence decays of DPA (cyan), G1 (orange) and G2 (green) in Argon-purged toluene. The excitation wavelength was 385 nm and emission was collected at 430 nm. The IRF shown in black was recorded using a fused silica plate and was about 60 ps (fwhm).

Table S1. Comparison of the fluorescence quantum yields (Φ_f), lifetimes (τ) and radiative rate constants (k_f) of DPA and the dendrimers.

	Φ_f	τ (ns)	k_f (s^{-1})
DPA	1.02[a]	7.0	$1.4 \cdot 10^8$
G1	1.03[a]	5.3	$1.9 \cdot 10^8$
G2	0.99	4.5	$2.2 \cdot 10^8$

a: The quantum yields for DPA and G1 appear to exceed unity but this is a mare effect of the real quantum yield being very close to unity in combination with minor measurement fluctuations.

3. Photolysis

Photolysis of DPA, G1 and G2 in toluene was performed using a handheld UV-lamp (UVP UVGL-25 Compact UV Lamp 4 W, 365 nm) by irradiating the samples with the energy flux of 2.7 mJ/s/cm^2. The peak of the lamp emission was found to be centered at 368 nm. Degradation of the samples was followed by measuring their absorption spectra using a CARY 5000 UV/Vis spectrometer.

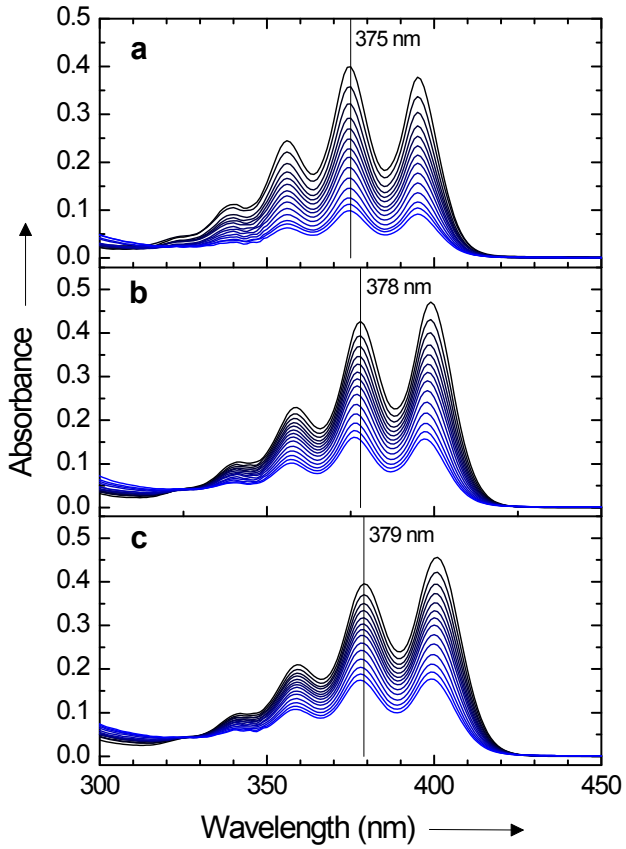

Figure S2. Absorption spectra of (a) DPA, (b) G1 and (c) G2 in toluene during UV-irradiation. Time-steps are as indicated in Figure S3.

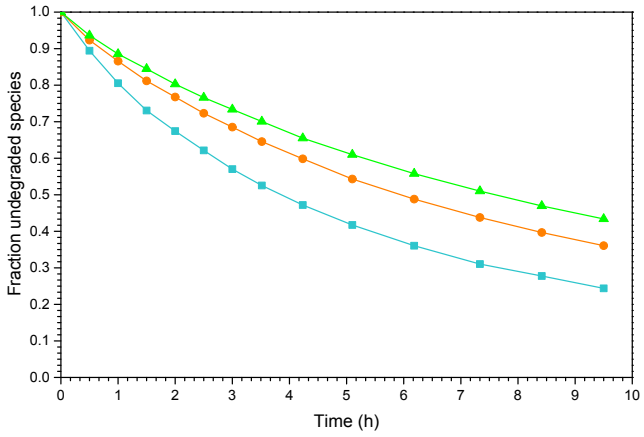

Figure S3. Degradation over time under UV-light exposure of DPA (cyan), G1 (orange) and G2 (green) in toluene. Degradation of the samples was measured by following the absorbance at 375 nm for DPA, 378 nm for G1 and 379 nm for G2.

4. Exciton models in the dendrimer systems

Two extreme cases for the exciton model in the dendrimers G1 and G2 can be distinguished: either a fully localized exciton or a delocalized exciton, illustrated in Figures S4 and S5 respectively.[3] In the figures the red arrows indicate the orientation of the transition dipole moments.

In the case of a fully localized exciton, each DPA unit acts as an individual chromophore as a result of a small intramolecular electronic coupling. Upon excitation, the excitation energy is initially localized on one DPA moiety and then may migrate over time to other parts of the molecule if the intramolecular electronic coupling is strong enough. As shown in Figure S4, excitation energy migration is accompanied by a change in the orientation of the emission dipole moment, which can cause depolarization and thus a decrease in the anisotropy according to the energy transfer rate.

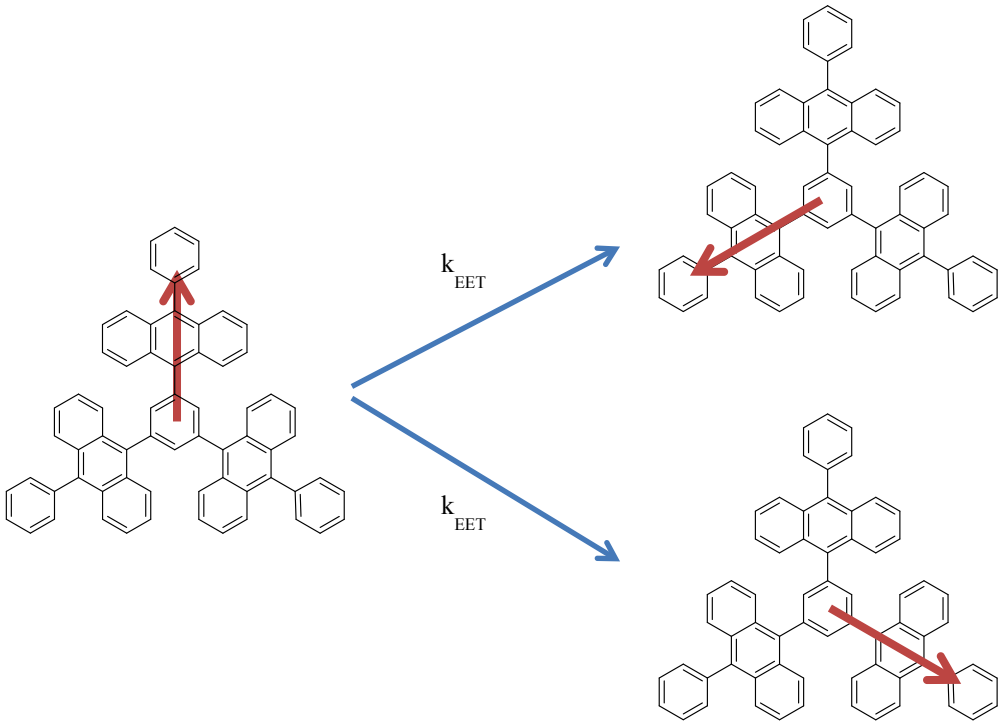

Figure S4. Localized excited states of the dendrimer G1. k_{EET} represents the excitation energy transfer rate constant.

The second case is a fully delocalized exciton upon excitation. Applied to the dendrimer G1, this results in the vector diagram shown in Figure S5. The transition moment is then given by the sum of the individual transition dipole moments. Three different combinations of the individual transition dipole moments are possible that leads to one transition forbidden (i.e. with a zero transition moment) and two allowed transitions for electric dipole transition from the ground state. Using the point dipole interaction to evaluate the energy of the three exciton states reveal that the forbidden exciton state is higher in energy, while the two allowed transitions are degenerate and lower in energy. Moreover upon symmetry lowering (i.e. removing the three-fold axis), these degenerate exciton states split in two perpendicular components as illustrated in Figure S6.

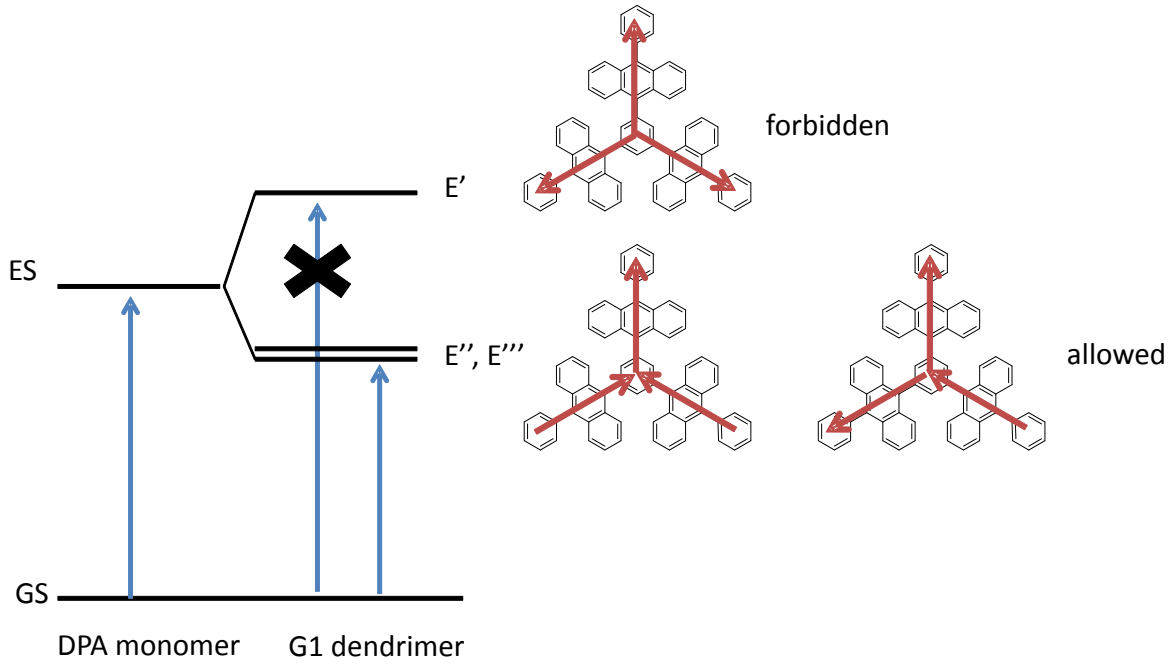

Figure S5. Exciton band energy diagram for the dendrimer G1 in the case of the fully delocalized exciton model.

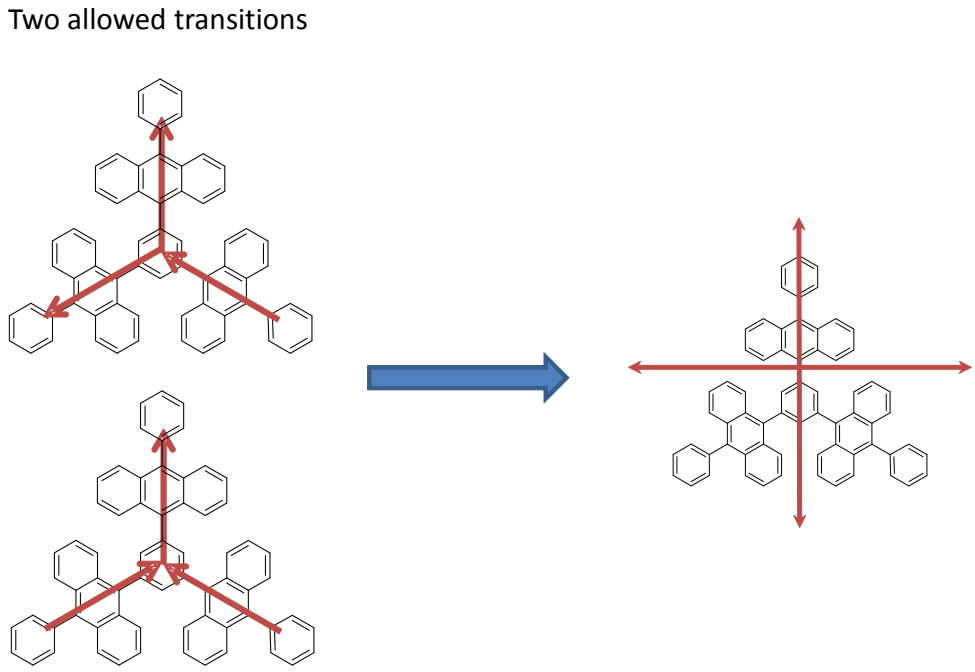

Figure S6. Splitting of the two allowed lowest electronic transitions into two perpendicular components upon symmetry lowering.

5. Quantum mechanical calculations

INDO/S calculations were made on the geometry optimized (AM1) structures of DPA, G1 and G2. The INDO/S calculations as implemented in the HyperChem 7.5 program were made with a configuration interaction using the 10 highest occupied and 10 lowest unoccupied molecular orbitals. The resulting lowest singlet-singlet transitions are shown in Figure S7. The agreement is quite reasonable and most importantly the lowest singlet electronic transition is always strong and with an energy that is independent of the size of the dendrimer. DPA has two electronic transitions in this low energy region; one strong (ν = 28 000 cm^{-1}, f = 0.5) and one weak (f = 0.05) at slightly higher energy. This is in accordance with earlier observations and with the decrease in fluorescence anisotropy with increasing excitation energy as seen in Figure 2. For G1 the two original transitions from DPA could in principle give rise to six new transitions but only the lowest pair have significant oscillator strength (both f = 0.7). The weaker higher energy transition in DPA is slightly blue shifted and splitted into three weak components. We believe that the two perpendicularly polarized lowest transitions dominate the first absorption band of G1. Please note that the qualitative conclusions from the QM calculation and the exciton coupling model are exactly the same. For G2 we expect more transitions and this is indeed observed in the calculated results. Still the lowest two electronic transitions are nearly degenerate and have a significant oscillator strength (f = 1.0).

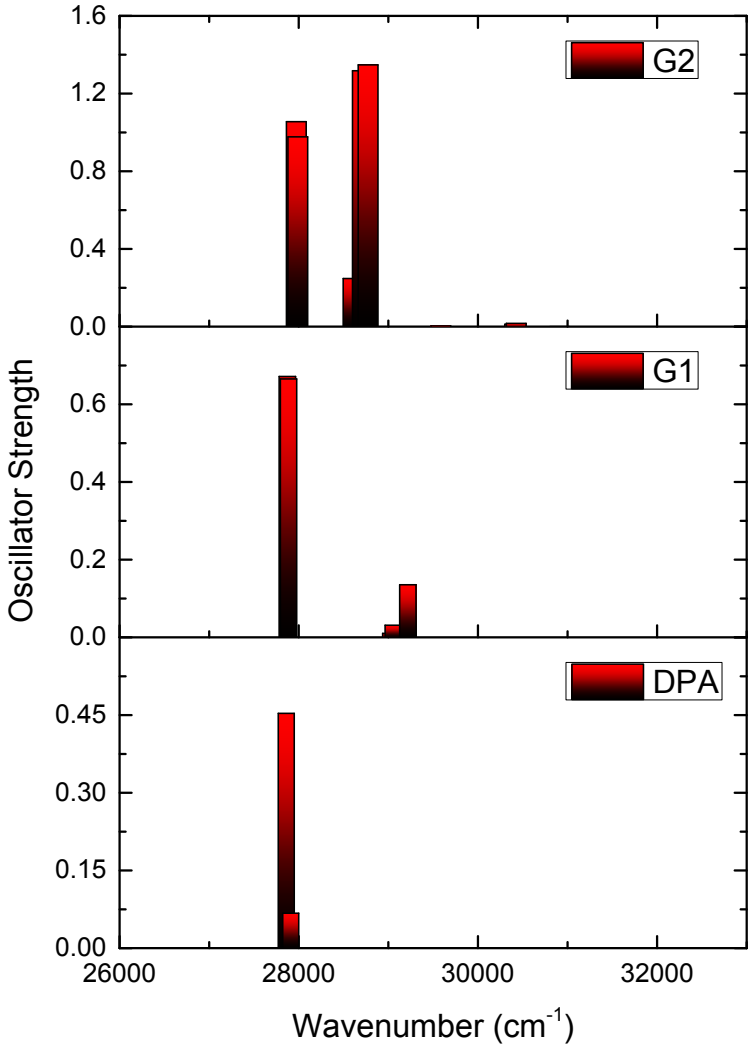

Figure S7. Calculated electronic transitions for DPA, G1 and G2 (INDO/S//AM1). Please observe that for G1 two equally strong (f=0.7) almost degenerate and perpendicular transitions overlap at 28000 cm^{-1}.

6. Steady-state fluorescence anisotropy

Steady-state anisotropy measurements provide information on the relative orientation of the absorption and emission dipole moments. Large anisotropy values close to 0.4 (maximum anisotropy value) indicate a parallel orientation of the absorption and emission dipole moments while low anisotropy values suggest a depolarization of the emission.[2] One common cause of depolarization is the rotation of the chromophore during the lifetime of its excited state, but also other processes such as energy transfer processes can lead to a depolarization of the emission.

In this work, anisotropy experiments were performed in freshly distilled 2-methyltetrahydrofuran (Sigma-Aldrich) which forms a glass around 90 K.[4] Steady-state excitation anisotropy spectra of DPA, G1 and G2 were recorded on a Spex Fluorolog 3 spectrofluorometer using Glan polarizers. Emission was measured at 415 nm for DPA and 430 nm for G1 and G2 while varying the excitation wavelength from 320 nm to 420 nm. The spectral bandwidths for the emission and excitation monochromators were 3 nm and 2 nm respectively. The anisotropy was calculated from the steady-state excitation spectra recorded at both vertical (V) and horizontal (H) polarization, using both vertically and horizontally polarized excitation (I_{VV}, I_{VH}, I_{HV} and I_{HH}).

$$r = \frac{I_{vv} - GI_{VH}}{I_{vv} + 2GI_{VH}} \qquad (2)$$

where G is an instrument-dependent factor, which corrects for the difference in sensitivity of the detection system to vertical and horizontal polarization, given by Eq 3.

$$G = \frac{I_{HV}}{I_{HH}} \qquad (3)$$

Studies of the temperature dependence of the steady-state anisotropy were performed using a temperature-controlled liquid nitrogen cooled cryostat (Oxford Instruments). Figure S8 shows the temperature dependence of the fundamental anisotropy for DPA, G1 and G2.

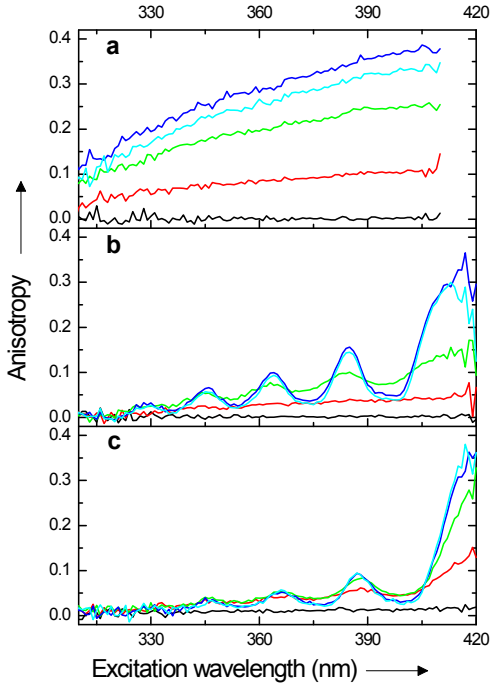

Figure S8. Steady-state fluorescence excitation anisotropy in 2-MTHF of (a) DPA at 295 K (black), 160 K (red), 140 K (green), 100 K (blue) and 80 K (cyan); (b) G1 at 295 K (black), 180 K (red), 140 K (green), 100 K (blue) and 80 K (cyan); (c) G2 at 295 K (black), 180 K (red), 140 K (green), 100 K (blue) and 80 K (cyan).

7. Resolution of absorption spectra from fluorescence excitation anisotropy spectra

At any excitation wavelength, the average anisotropy follows an additive law and can be expressed as the sum of anisotropies of individual states or species.[5]

$$r_0(\lambda) = f_a(\lambda) r_{0,a} + f_b(\lambda) r_{0,b} \quad (4)$$

$$f_a(\lambda) + f_b(\lambda) = 1 \quad (5)$$

Where $f_i(\lambda)$ represents the fractional contribution of the state *i* to the total anisotropy and $r_{0,i}$ corresponds to the fundamental anisotropy of this state. In Eq 4, $r_{0,a}$ and $r_{0,b}$ are assumed to be independent of the wavelength.

In the case of G1, if we assume two perpendicular major transitions (Figure S6) in the lowest absorption band of G1 with one of them having a limiting anisotropy of 0.3 (the maximum value observed), the lowest lying transition can be spectrally resolved with the help of the steady-state fluorescence excitation anisotropy using the following equations. By assigning the highest value of r_0 to $r_{0,a}$, one obtains $r_{0,b}$=-0.15 according to Eq 6.[2]

$$r_{0,b} = 0.3\left(\frac{3cos^2\beta - 1}{2}\right) \quad (6)$$

where β represents the angle between the absorption and emission transition dipoles. Here β is equal to 90° as we made the assumption, supported by theory and calculations, that the two lowest electronic transitions are perpendicular. Now, using Eqs. 4 and 5, the fractional contribution of each transition to the total anisotropy or absorption is directly obtained from the measured steady-state excitation anisotropy yielding Eqs. 7 and 8.

$$f_a(\lambda) = \frac{r_0(\lambda) + 0.15}{0.45} \quad (7)$$

$$f_b(\lambda) = \frac{0.3 - r_0(\lambda)}{0.45} \quad (8)$$

Finally the respective absorption spectra of the transitions *a* and *b* are calculated using the following equations.

$$A_a(\lambda) = A(\lambda) f_a(\lambda) \quad (9)$$

$$A_b(\lambda) = A(\lambda) f_b(\lambda) \quad (10)$$

8. Time-resolved fluorescence anisotropy

Time-resolved fluorescence anisotropy can provide information on the nature of the depolarization channels: for example, rotational motion of the chromophore or excitation energy transfer. In the case of rotational motion of the chromophore as the unique depolarization channel such as DPA, following excitation with a linearly polarized light pulse the fluorescence anisotropy *r(t)* for a sphere decays mono-exponentially according to Eq. 11.

$$r(t) = r_0 e^{-t/\theta} \qquad (11)$$

Where r_0 is the anisotropy at time zero and θ represents the rotational correlation time of the chromophore. But depolarization can also result from excitation energy transfer processes if these are accompanied by a change in the direction of the transition dipole moments. In the presence of both rotational depolarization (for a sphere) and excitation energy transfer the decay of the fluorescence anisotropy will be double exponential:

$$r(t) = r_{0,a} e^{-t/\theta_a} + r_{0,b} e^{-t/\theta_b} \qquad (12)$$

To investigate the presence of excitation energy transfer in the dendrimers G1 and G2 and distinguish this process from rotational motions of the chromophore, fluorescence anisotropy decays of G1 and G2 were measured as function of the temperature. The fluorescence anisotropy decay of DPA, in which no excitation energy migration can occur, was also measured as function of temperature and compared to the ones of the dendrimers. Experimentally time-resolved fluorescence anisotropy was measured using the TCSPC set up described previously (see section 2). The excitation wavelength was set at 385 or 395 nm as previously and photons were collected at 430 nm with a spectral band width of 6-10 nm. The signal was digitalized using a multi-channel analyzer with 4096 channels (SPC-300, Edinburgh Analytical Instruments) and was recorded for 5 min corresponding to at least 10 000 counted photons in the top channel. Fluorescence decays $I_{VV}(t)$ and $I_{VH}(t)$ were measured with the polarization of the detection parallel or perpendicular respectively to the polarization of the excitation pulse (vertically polarized). The anisotropy decay was then calculated according to the following formula:

$$r(t) = \frac{I_{VV}(t) - GI_{VH}(t)}{I_{VV}(t) + 2GI_{VH}(t)} \qquad (13)$$

The correction factor G was obtained by $I_{HV}(t)/I_{HH}(t)$ where $I_{HV}(t)$ and $I_{HH}(t)$ are the fluorescence decays with the polarization of the detection perpendicular or parallel respectively to the polarization of the excitation pulse (horizontally polarized). To rotate the plane of polarization of the excitation pulse from vertical to horizontal, a Berek polarization compensator (Model 5540) that acts as a half-wave plate was placed on the excitation path before the sample. Finally the anisotropy decays were fitted to mono-exponential or bi-exponential expressions using the program AniFit – Anisotropy Decay Analysis 1.1 (Fluortools, www.fluortools.com) after deconvolution of the data with the instrument response function (IRF). In the fitting procedure, as G was found to be time-independent, an averaged value of G was used.

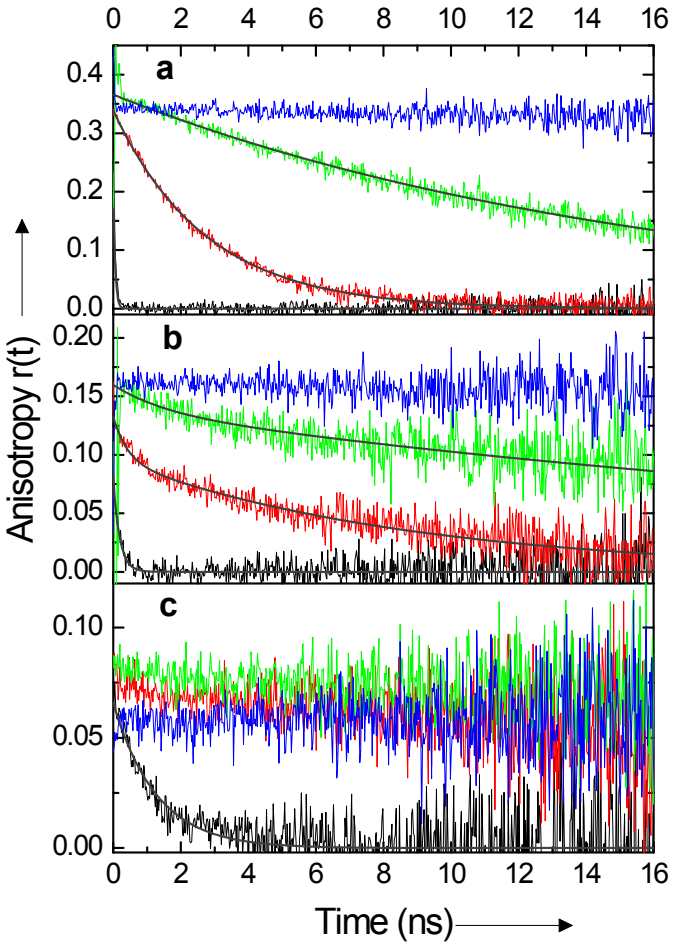

Figure S9. Time-resolved fluorescence anisotropy decays of (a) DPA, (b) G1 and (c) G2 at 300 K (black), 160 K (red), 140 K (green) and 100 K (blue) in 2-MTHF. The excitation wavelength was 385 nm and photons were collected at 430 nm.

Table S2. Fitted fluorescence anisotropy decay parameters of DPA, G1 and G2 excited at 385 nm in 2-MTHF.

Sample	Temperature	$r_{0,a}$	θ_a (ns)	$r_{0,b}$	θ_b (ns)	θ_{calc} (ns)[a]	τ (ns)	χ^2
DPA								
	300 K	0.23	0.05	-	-	0.06	5.5	1.653
	160 K	0.34	2.7	-	-	2.3	6.8	1.681
	140 K	0.36	15.6	-	-	13.0	6.8	1.278
	100 K	0.34	>100	-	-	$>10^7$	7.5	N.A
G1								
	300 K	0.08	0.19	-	-	0.15	4.3	1.907
	160 K	0.04	0.42	0.09	8.6	5.8	5.2	1.516
	140 K	0.02	1.5	0.14	34	32.8	5.2	1.187
	100 K	0.16[b]	>100	-	-	$>10^7$	5.4	N.A
G2								
	300 K	0.07	1.3	-	-	0.43	3.5	2.285
	160 K	0.08[b]	>100	-	-	16.3	3.5	N.A
	140 K	0.08[b]	>100	-	-	92.3	3.9	N.A
	100 K	0.04[b]	>100	-	-	$> 10^7$	N.A	N.A

[a] The rotational correlation time θ_{calc} is estimated using the equation $\theta_{calc} = \eta V / k_b T$ where η is the viscosity of 2-MTHF at the temperature T, V is the volume of the rotating fluorophore[6] and k_b is the Boltzmann constant. For G1 and G2, the volume of the rotating unit was assumed to scale up linearly with the molecular mass, taking the molecular mass of DPA as a reference. [b] The $r_{0,a}$ values are the values read at time zero on the raw data and are not estimation from any fitting.

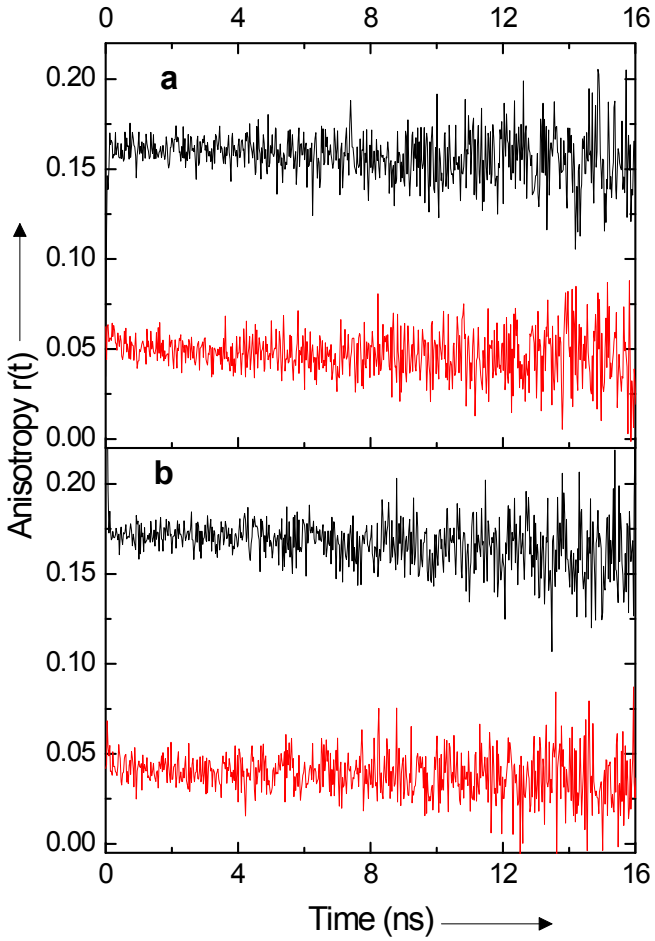

Figure S10. Time-resolved fluorescence anisotropy decays of G1 at (a) 100 K and (b) 80 K, excited at 385 nm (black) and at 395 nm (red).

9. Estimation of Förster Resonance Energy Transfer rates

The time for homo-Förster Resonance Energy Transfer between the DPA chromophores over the longest distances in the dendrimers, as indicated in Figure S11, are found in Table S3. The longest distance energy transfer scenario estimated for G2 certainly is least likely to occur but the estimate serves the purpose as a bench-mark for the longest possible energy transfer time in this overly simplified model. In reality many shorter transfer times, including multiple hop events will give rise to very complex anisotropy decay.

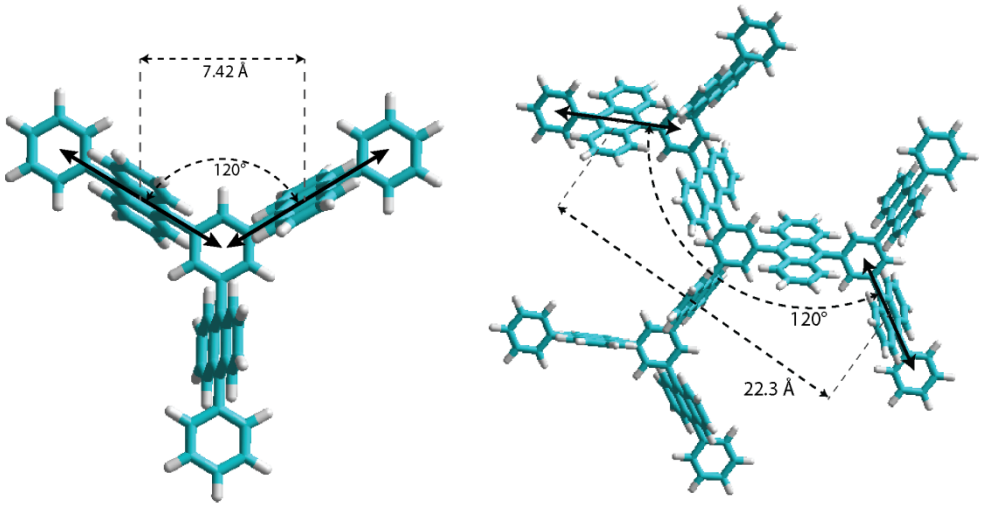

Figure S11. The relative orientations of DPA chromophores in G1 (left) and for the longest distance in G2 (right).

Table S3: Transfer times for Homo-FRET between DPA chromophores in the two dendrimers over the given distances.

	G1	G2
Distance r (Å)	7.4Å	22 Å
τ_T=1/k_T(r) (s)	$36 \cdot 10^{-15}$	$27 \cdot 10^{-12}$

The overlap integral ($J(\lambda)$)[7] was calculated to $2.4 \cdot 10^{13}$ nm^4/(M cm) for DPA-to-DPA FRET. Further calculations[2] were conducted as follows; the FRET orientation factor kappa squared is

$$\kappa^2 = (\cos(\theta_T) - 3cos(\theta_D)cos(\theta_A))^2 \quad (14)$$

where θ_T =120°, θ_D =30°, and θ_A =150° yielded κ^2 = 3.0625. The characteristic FRET distance, R_0 was estimated through

$$R_0 = 0.211(\kappa^2 n^4 Q_D J(\lambda))^{1/6} (in \text{ Å}) \quad (15)$$

where n= 1.496 is the refractive index of toluene and Q_D = 1 is the quantum yield of the donor. The energy transfer rate was calculated as

$$k_T(r) = \frac{1}{\tau_D}\left(\frac{R_0}{r}\right)^6 \quad (16)$$

where τ_D= 7 ns is the lifetime of DPA under Ar-purged conditions. Inversion of the rate constant gives the transfer time as τ_T=1/k_T(r) (s).

10. Molar Absorptivities

Table S4. Molar absorptivities of the studied compounds in toluene.

	Molar absorptivity (M^{-1} cm^{-1})	**Wavelength (nm)**
DPA	12 500	375
G1	49 000	399
G2	110 000	401

References

[1] K. Suzuki, A. Kobayashi, S. Kaneko, K. Takehira, T. Yoshihara, H. Ishida, Y. Shiina, S. Oishi, S. Tobita, *Physical Chemistry Chemical Physics* **2009**, *11*, 9850.

[2] J. R. Lakowicz, *Principles of Fluorescence Spectroscopy. Third Edition*, Springer, New-York, NY, **2006**.

[3] M. Kasha, *Reviews of Modern Physics* **1959**, *31*, 162.

[4] B. Brocklehurst, R. N. Young, *Journal of the Chemical Society, Faraday Transactions* **1994**, *90*, 271.

[5] B. Valeur, G. Weber, *Photochemistry and Photobiology* **1977**, *25*, 441.

[6] B. S. Johnson, M. D. Ediger, Y. Yamaguchi, Y. Matsushita, I. Noda, *Polymer* **1992**, *33*, 3916.

[7] a|e - UV-Vis-IR Spectral Software 1.2`, FluorTools`, www.fluortools.com